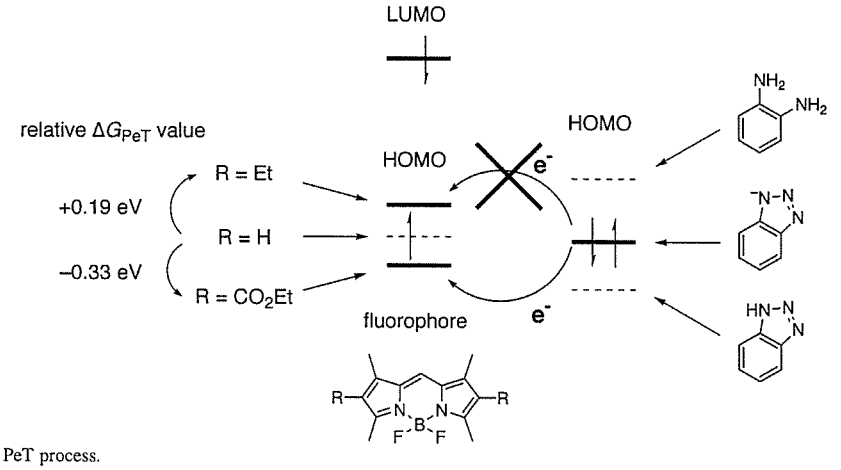

Figure 8. Schematic PeT process.

Scheme 5. Synthetic Scheme of DAMBO-Rs

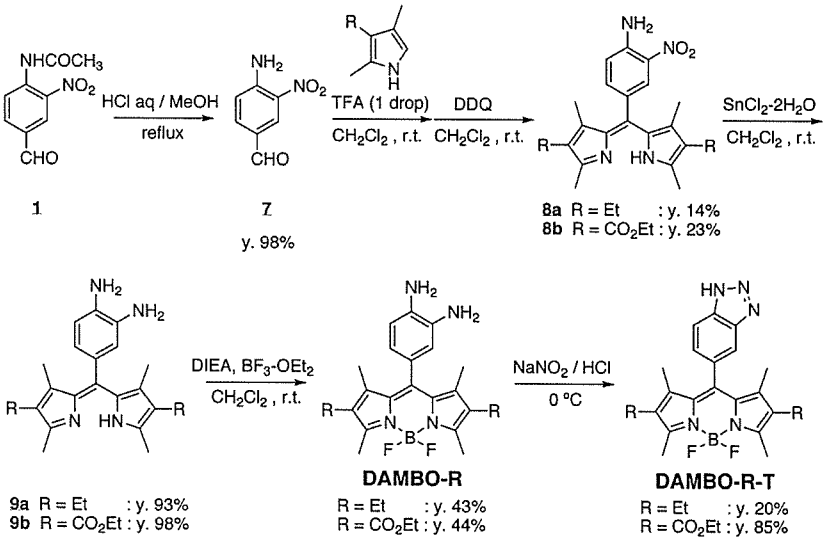

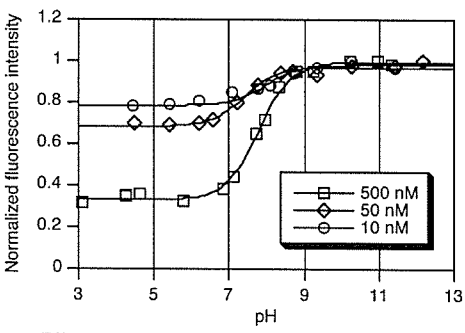

Figure 9. Effect of pH on the fluorescence intensity of DAMBO-Et-T (0.5% DMSO as a cosolvent) in sodium phosphate buffer (0.1 M). The fluorescence intensities were determined at 535 nm with excitation at 520 nm.

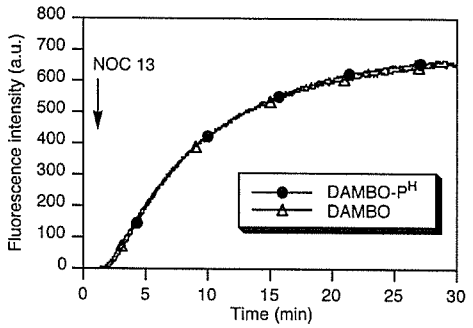

Figure 10. Fluorescence increase with DAMBOs (5 μM, 0.1% DMSO) upon reaction with NOC 13 (20 μM) in 0.1 M sodium phosphate buffer (pH 7.4). The fluorescence intensities of DAMBO-P^H and DAMBO were determined at 535 and 512 nm with excitation at 520 and 495 nm, respectively. NOC 13 was added at the point indicated by the arrow.

DAMBO-P^H and DAMBO were almost the same (Figure 10). We thus succeeded in the development of a highly sensitive and pH-independent NO probe, DAMBO-P^H.

Very recently, Zhang et al. reported a compound whose proposed structure was the same as that of one of our DAMBO derivatives.[21] However, their compounds were not well characterized, and the fluorescence properties were in marked

(21) Zhang, X.; Wang, H.; Li, J.-S.; Zhang, H.-S. *Anal. Chem. Acta* **2003**, *481*, 101–108.

Scheme 6. Synthetic Scheme of DAMBO-P^Hs

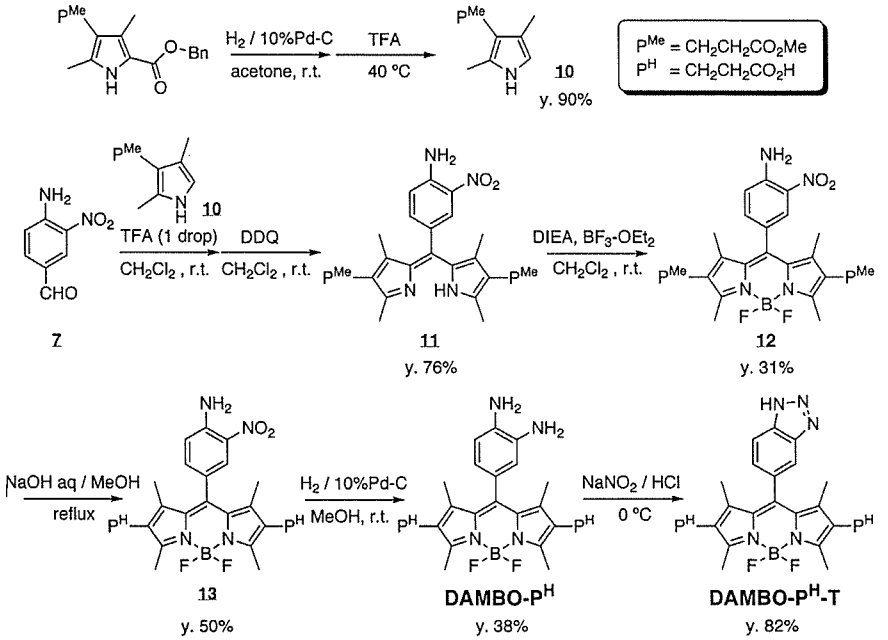

contrast to those of our compounds. We characterized our compounds in detail by means of ^1H NMR, ^{13}C NMR, high-resolution mass spectroscopy, and elemental analysis, and their fluorescence properties could be well interpreted in terms of PeT theory. Moreover, other diamino BODIPYs reported in this paper also showed fluorescence properties similar to those of DAMBO, so we consider that DAMBO and its derivatives are novel fluorescence probes for NO.

The probe, DAMBO-P^H, can be used in buffer solution, so it should be potentially useful for detection of NO in biological applications.

Conclusion

BODIPY is a well-known chromophore that is highly fluorescent in almost all solvents but has not been utilized much in biological functional probes.

We found that the fluorescence properties of BODIPYs can be controlled through a PeT-dependent fluorescence off/on switching mechanism, and we succeeded in developing DAMBO-P^H as a sensitive probe for NO, based on the following strategy: (1) raising the electron density of the reaction site in order to acquire higher sensitivity for NO, (2) optimizing the PeT process by modulating the spectroscopic and electrochemical properties of the BODIPY chromophore to avoid the pH dependency of fluorescence intensity in the pH region of biological interest, and (3) introducing carboxyl functional groups to increase hydrophilicity, thereby preventing the quenching of fluorescence by stacking. Further studies on biological applications of DAMBO-P^H are in progress.

A similar rational design strategy may also be applicable to other fluorophores, such as cyanine dye, in addition to BODIPY, for the development of various biofunctional and practical fluorescence probes.

Experimental Section

Materials. General chemicals were of the best grade available, supplied by Tokyo Chemical Industries, Wako Pure Chemical, or Aldrich Chemical Co., and used without further purification. Special chemicals were dimethyl sulfoxide (DMSO, fluorometric grade, Dojindo) and tetrabutylammonium perchlorate (TBAP, electrochemical grade, dried over P_2O_5 before use, Fluka). All solvents were used after appropriate distillation or purification.

Instruments. NMR spectra were recorded on a JEOL JNM-LA300 instrument at 300 MHz for ^1H NMR and at 75 MHz for ^{13}C NMR. Mass spectra (MS) were measured with a JEOL SX-102A for EI and a JEOL JMS-T100LC AccuTOF for ESI. UV−visible spectra were obtained on a Shimadzu UV-1600. Fluorescence spectroscopic studies were performed on a Hitachi F4500. Determinations of pH profile of fluorescence and time course of fluorescence increase upon reaction with NO were performed on a Perkin-Elmer LS-50B.

Synthesis of 4-Acetamido-3-nitrobenzaldehyde (1). Fuming nitric acid (1.0 mL) was carefully added dropwise to concentrated sulfuric acid (6 mL) at 0 °C. 4-Acetamidobenzaldehyde (1.91 g, 11.7 mmol) was added to the solution at 0 °C. At the end of addition, the reaction mixture was poured onto ice. The precipitated yellow powder was collected by filtration, washed with cold water, dried, purified by silica gel chromatography (CH_2Cl_2), and recrystallized from water to afford light yellow needles (1.57 g, yield 64%). ^1H NMR ($CDCl_3$): δ 2.36 (s, 3H); 8.16 (dd, 1H, J = 1.7, 8.8 Hz); 8.74 (d, 1H, J = 1.7 Hz); 9.04 (d, 1H, J = 8.8 Hz); 9.99 (s, 1H); 10.63 (s, 1H). MS (EI): 208 (M^+). Mp: 156 °C.

Synthesis of 6-(4-Acetamido-3-nitrophenyl)-3,3′,5,5′-tetramethylpyrromethene (2). 1 (953 mg, 4.58 mmol) and 2,4-dimethylpyrrole (0.94 mL, 9.16 mmol) were dissolved in 250 mL of absolute CH_2Cl_2 under an Ar atmosphere. One drop of trifluoroacetic acid (TFA) was added, and the solution was stirred at room temperature overnight. When TLC monitoring (silica; CH_2Cl_2) showed complete consumption of the aldehyde, a solution of 2,3-dichloro-5,6-dicyano-1,4-benzoquinone (DDQ) (1.07 g, 4.58 mmol) in CH_2Cl_2 was added, and stirring was continued for 15 min. The reaction mixture was washed with water, dried over $MgSO_4$, filtered, and evaporated. The crude compound was purified by column chromatography on aluminum oxide (CH_2Cl_2) to afford a brown powder (442 mg, yield 26%). ^1H NMR ($CDCl_3$): δ 1.35 (s, 6H); 2.33 (s, 3H); 2.35 (s, 6H); 5.91 (s, 2H); 7.60 (dd, 1H, J = 2.0, 8.6 Hz); 8.20 (d, 1H, J = 2.0 Hz); 8.93 (d, 1H, J = 8.6 Hz); 10.46 (s, 1H). HRMS (EI^+): calcd for M^+, 378.1692; found, 378.1696.

Synthesis of 6-(4-Amino-3-nitrophenyl)-3,3′,5,5′-tetramethylpyrromethene (3). 2 (285 mg, 0.75 mmol) was dissolved in 20 mL of MeOH, then 20 mL of 1 N HCl was added, and the mixture was refluxed at 100 °C for 1 h. The reaction mixture was neutralized with 2 N NaOH. The aqueous solution was extracted with CH_2Cl_2. The combined organic extracts were dried over Na_2SO_4, filtered, and evaporated to afford a brown powder (250 mg, yield 99%). ^{1}H NMR ($CDCl_3$): δ 1.46 (s, 6H); 2.34 (s, 6H); 5.91 (s, 2H); 6.17 (s, 2H); 6.90 (d, 1H, J = 8.4 Hz); 7.29 (dd, 1H, J = 1.8, 8.4 Hz); 8.09 (d, 1H, J = 1.8 Hz). HRMS (EI$^+$): calcd for M$^+$, 336.1586; found, 336.1614.

Synthesis of 6-(3,4-Diaminophenyl)-3,3′,5,5′-tetramethylpyrromethene (4). 3 (250 mg, 0.74 mmol) was dissolved in 50 mL of CH_2Cl_2 saturated with concentrated HCl. The solution was stirred at 0 °C for 20 min, then $SnCl_2$–$2H_2O$ (3.35 g, 14.9 mmol) was added, and stirring was continued at room temperature overnight. When TLC monitoring (alumina; CH_2Cl_2/MeOH, 9:1) showed complete consumption of **3**, the reaction mixture was washed with 2 N NaOH. The aqueous solution was extracted with CH_2Cl_2. The combined organic extracts were dried over Na_2SO_4, filtered, and evaporated to afford a light brown powder (215 mg, yield 95%). ^{1}H NMR ($CDCl_3$): δ 1.46 (s, 6H); 2.33 (s, 6H); 3.39 (s, 2H); 3.49 (s, 2H); 5.89 (s, 2H); 6.62 (dd, 1H, J = 1.8, 8.3 Hz); 6.63 (d, 1H, J = 1.8 Hz); 6.75 (d, 1H, J = 8.3 Hz). HRMS (EI$^+$): calcd for M$^+$, 306.1844; found, 306.1843.

Synthesis of 8-(3,4-Diaminophenyl)-4,4-difluoro-1,3,5,7-tetramethyl-4-bora-3a,4a-diaza-*s*-indacene (DAMBO). 4 (129 mg, 0.42 mmol) and *N,N*-diisopropylethylamine (DIEA) (1.0 mL, 5.7 mmol) were dissolved in 20 mL of absolute CH_2Cl_2 under an Ar atmosphere, and the solution was stirred at room temperature for 10 min. BF_3–OEt_2 (1.0 mL, 7.9 mmol) was added, and stirring was continued for 40 min. The reaction mixture was washed with water and 2 N NaOH. The aqueous solution was extracted with CH_2Cl_2. The combined organic extracts were dried over Na_2SO_4, filtered, and evaporated. The crude compound was purified by column chromatography over aluminum oxide (CH_2Cl_2/MeOH, 20:1) and recrystallized from $CHCl_3$/*n*-hexane to afford orange crystals (105 mg, yield 71%). ^{1}H NMR ($CDCl_3$): δ 1.53 (s, 6H); 2.54 (s, 6H); 3.44 (s, 2H); 3.52 (s, 2H); 5.96 (s, 2H); 6.58 (d, 1H, J = 8.4 Hz); 6.59 (s, 1H); 6.79 (d, 1H, J = 8.4 Hz). ^{13}C NMR ($CDCl_3$): δ 14.6, 14.6, 116.0, 117.0, 119.8, 120.8, 126.5, 131.9, 135.4, 135.4, 142.7, 143.3, 154.9. HRMS (EI$^+$): calcd for M$^+$, 354.1827; found, 354.1838. Mp: 251–254 °C (dec). Anal. Calcd for $C_{19}H_{21}BF_2N_4$: C, 64.43; H, 5.98; N, 15.82. Found: C, 64.40; H, 5.92; N, 15.61.

Synthesis of 8-(5-Benzotriazolyl)-4,4-difluoro-1,3,5,7-tetramethyl-4-bora-3a,4a-diaza-*s*-indacene (DAMBO-T). An aqueous solution of $NaNO_2$ (10 mg, 0.15 mmol) was added to a suspension of **DAMBO** (50 mg, 0.14 mmol) in 25 mL of 2 N HCl at 0 °C. The mixture was stirred at room temperature for 15 min. The resulting mixture was extracted with CH_2Cl_2. The combined organic extracts were dried over Na_2SO_4, filtered, and evaporated. The crude compound was purified by preparative reversed-phase HPLC (ODS, eluent: CH_3CN/H_2O/TFA, 50:50:0.1) and recrystallized from $CHCl_3$ to afford orange crystals (15 mg, yield 29%). ^{1}H NMR ($CDCl_3$): δ 1.26 (s, 6H); 2.57 (s, 6H); 5.99 (s, 2H); 7.41 (d, 1H, J = 8.4 Hz); 7.87 (s, 1H); 8.07 (d, 1H, J = 8.4 Hz). HRMS (EI$^+$): calcd for M$^+$, 365.1623; found, 365.1630. Mp: 282–286 °C (dec).

Synthesis of 4,4′-Diethyl-3,3′,5,5′-tetramethyl-6-phenylpyrromethene (5a), 4,4′-Diethoxycarbonyl-3,3′,5,5′-tetramethyl-6-phenylpyrromethene (5b), and 3,3′,5,5′-Tetramethyl-6-phenylpyrromethene (5c). Benzaldehyde (0.10 mL, 1.0 mmol) and 2,4-dimethyl-3-ethylpyrrole (0.27 mL, 2.0 mmol) were dissolved in 50 mL of absolute CH_2Cl_2 under an Ar atmosphere. One drop of TFA was added, and the solution was stirred at room temperature overnight. When TLC monitoring (silica; CH_2Cl_2) showed complete consumption of the aldehyde, a solution of DDQ (234 mg, 1.0 mmol) in CH_2Cl_2 was added, and stirring was continued for 15 min. The reaction mixture was washed with water, dried over $MgSO_4$, filtered, and evaporated. The crude compound was purified by column chromatography over aluminum oxide (CH_2Cl_2) to afford a brown powder (138 mg, yield 42%). ^{1}H NMR ($CDCl_3$): δ 0.97 (t, 6H, J = 7.5 Hz); 1.19 (s, 6H); 2.27 (q, 4H, J = 7.5 Hz); 2.32 (s, 6H); 7.29–7.33 (m, 2H); 7.38–7.42 (m, 3H); 13.10 (s, 1H). HRMS (EI$^+$): calcd for M$^+$, 332.2252; found, 332.2263.

5b and **5c** were similarly prepared from ethyl 2,4-dimethylpyrrole-3-carboxylate[22] and 2,4-dimethylpyrrole in 63% and 39% yield, respectively.

5b. ^{1}H NMR ($CDCl_3$): δ 1.32 (t, 6H, J = 7.1 Hz); 1.59 (s, 6H); 2.59 (s, 6H); 4.25 (q, 4H, J = 7.1 Hz); 7.28–7.32 (m, 2H); 7.46–7.48 (m, 3H). HRMS (EI$^+$): calcd for M$^+$, 420.2049; found, 420.2079.

5c. ^{1}H NMR ($CDCl_3$): δ 1.29 (s, 6H); 2.34 (s, 6H); 5.88 (s, 2H); 7.28–7.31 (m, 2H); 7.40–7.42 (m, 3H). HRMS (EI$^+$): calcd for M$^+$, 276.1626; found, 276.1642.

Synthesis of 2,6-Diethyl-4,4-difluoro-1,3,5,7-tetramethyl-8-phenyl-4-bora-3a,4a-diaza-*s*-indacene (6a), 2,6-Diethoxycarbonyl-4,4-difluoro-1,3,5,7-tetramethyl-8-phenyl-4-bora-3a,4a-diaza-*s*-indacene (6b), and 4,4-Difluoro-1,3,5,7-tetramethyl-8-phenyl-4-bora-3a,4a-diaza-*s*-indacene (6c). 5a (109 mg, 0.33 mmol) and DIEA (2.0 mL, 11.5 mmol) were dissolved in 100 mL of absolute CH_2Cl_2 under an Ar atmosphere and stirred at room temperature for 10 min. BF_3–OEt_2 (2.0 mL, 15.8 mmol) was added, and stirring was continued for 1 h. The reaction mixture was washed with water and 2 N NaOH. The aqueous solution was extracted with CH_2Cl_2. The combined organic extracts were dried over Na_2SO_4, filtered, and evaporated. The crude compound was purified by silica gel chromatography (CH_2Cl_2/*n*-hexane, 2:1) and recrystallized from *n*-hexane to afford orange needles (118 mg, yield 95%). ^{1}H NMR ($CDCl_3$): δ 0.98 (t, 6H, J = 7.7 Hz); 1.27 (s, 6H); 2.30 (q, 4H, J = 7.7 Hz); 2.53 (s, 6H); 7.26–7.30 (m, 2H); 7.46–7.48 (m, 3H). ^{13}C NMR ($CDCl_3$): δ 11.6, 12.5, 14.6, 17.0, 128.2, 128.7, 129.0, 130.8, 132.7, 135.8, 138.4, 140.2, 153.6. HRMS (EI$^+$): calcd for M$^+$, 380.2235; found, 380.2245. Mp: 185–186 °C. Anal. Calcd for $C_{23}H_{27}BF_2N_2$: C, 72.64; H, 7.16; N, 7.37. Found: C, 72.66; H, 7.16; N, 7.26.

6b and **6c** were similarly prepared from **5b** and **5c** in 10% and 78% yield, respectively.

6b. Recrystallized from $CHCl_3$/*n*-hexane to afford orange needles. ^{1}H NMR ($CDCl_3$): δ 1.32 (t, 6H, J = 7.1 Hz); 1.66 (s, 6H); 2.84 (s, 6H); 4.28 (q, 4H, J = 7.1 Hz); 7.26–7.29 (m, 2H); 7.53–7.55 (m, 3H). ^{13}C NMR ($CDCl_3$): δ 13.6, 14.3, 15.0, 60.2, 122.6, 127.7, 129.6, 129.7, 131.4, 134.4, 145.8, 147.7, 159.5, 164.3. HRMS (EI$^+$): calcd for M$^+$, 468.2032; found, 468.2035. Mp: 204–205 °C. Anal. Calcd for $C_{25}H_{27}BF_2N_2O_4$: C, 64.12; H, 5.81; N, 5.98. Found: C, 63.99; H, 5.81; N, 5.97.

6c. Recrystallized from $CHCl_3$/*n*-hexane to afford green crystals. ^{1}H NMR ($CDCl_3$): δ 1.37 (s, 6H); 2.56 (s, 6H); 5.98 (s, 2H); 7.27–7.30 (m, 2H); 7.47–7.49 (m, 3H). ^{13}C NMR ($CDCl_3$): δ 14.3, 14.6, 121.2, 127.9, 128.9, 129.1, 131.4, 135.0, 141.7, 143.1, 155.4. HRMS (EI$^+$): calcd for M$^+$, 324.1609; found, 324.1596. Mp: 176–177 °C. Anal. Calcd for $C_{19}H_{19}BF_2N_2$: C, 70.39; H, 5.91; N, 8.64. Found: C, 70.67; H, 6.00; N, 8.82.

Synthesis of 4-Amino-3-nitrobenzaldehyde (7). 1 (2.08 g, 10 mmol) was dissolved in 200 mL of MeOH, then 50 mL of 2 N HCl was added, and the mixture was refluxed at 80 °C for 8 h under an Ar atmosphere. The reaction mixture was evaporated and washed with 2 N NaOH. The aqueous solution was extracted with CH_2Cl_2. The combined organic extracts were dried over Na_2SO_4, filtered, and evaporated to afford yellow needles (1.62 g, yield 98%). ^{1}H NMR ($CDCl_3$): δ 6.91 (1H, d, J = 8.6 Hz); 7.92 (dd, 1H, J = 2.0, 8.6 Hz); 8.63 (d, 1H, J = 2.0 Hz); 9.82 (s, 1H). MS (EI): 166 (M$^+$).

Synthesis of 6-(4-Amino-3-nitrophenyl)-4,4′-diethyl-3,3′,5,5′-tetramethylpyrromethene (8a) and 6-(4-Amino-3-nitrophenyl)-4,4′-diethoxycarbonyl-3,3′,5,5′-tetramethylpyrromethene (8b). 7 (424 mg,

(22) Alberola, A.; Ortega, A. G.; Sádaba, M. L.; Sañudo, C. *Tetrahedron* **1999**, *55*, 6555–6566.

2.5 mmol) and 2,4-dimethyl-3-ethylpyrrole (616 mg, 5.0 mmol) were dissolved in 100 mL of absolute CH_2Cl_2 under an Ar atmosphere. One drop of TFA was added, and the solution was stirred at room temperature overnight. A solution of DDQ (585 mg, 2.5 mmol) in CH_2Cl_2 was added, and stirring was continued for 15 min. The reaction mixture was washed with water, dried over $MgSO_4$, filtered, and evaporated. The crude compound was purified by column chromatography over aluminum oxide (CH_2Cl_2) to afford a brown powder (136 mg, yield 14%). ^{1}H NMR ($CDCl_3$): δ 0.98 (t, 6H, J = 7.5 Hz); 1.35 (s, 6H); 2.29 (q, 4H, J = 7.5 Hz); 2.31 (s, 6H); 6.17 (s, 2H); 6.89 (d, 1H, J = 8.6 Hz); 7.30 (dd, 1H, J = 2.0, 8.6 Hz); 8.09 (d, 1H, J = 2.0 Hz). HRMS (EI$^+$): calcd for M$^+$, 392.2212; found, 392.2200.

8b was similarly prepared from ethyl 2,4-dimethylpyrrole-3-carboxylate in 23% yield. ^{1}H NMR ($CDCl_3$): δ 1.33 (t, 6H, J = 7.1 Hz); 1.77 (s, 6H); 2.58 (s, 6H); 4.26 (q, 4H, J = 7.1 Hz); 6.28 (s, 2H); 6.95 (d, 1H, J = 8.6 Hz); 7.27 (d, 1H, J = 8.6 Hz); 8.08 (s, 1H). HRMS (EI$^+$): calcd for M$^+$, 480.2009; found, 480.1983.

Synthesis of 6-(3,4-Diaminophenyl)-4,4′-diethyl-3,3′,5,5′-tetramethylpyrromethene (9a) and 6-(3,4-Diaminophenyl)-4,4′-diethoxycarbonyl-3,3′,5,5′-tetramethylpyrromethene (9b). **9a** and **9b** were prepared from **8a** and **8b** by the same method as that used to obtain **4**, in 93% and 98% yield, respectively.

9a. ^{1}H NMR ($CDCl_3$): δ 0.98 (t, 6H, J = 7.5 Hz); 1.35 (s, 6H); 2.29 (q, 4H, J = 7.5 Hz); 2.30 (s, 6H); 3.39 (s, 2H); 3.50 (s, 2H); 6.63 (dd, 1H, J = 1.5, 8.3 Hz); 6.64 (d, 1H, J = 1.5 Hz); 6.74 (d, 1H, J = 8.3 Hz). HRMS (EI$^+$): calcd for M$^+$, 362.2470; found, 362.2472.

9b. ^{1}H NMR ($CDCl_3$): δ 1.32 (t, 6H, J = 7.1 Hz); 1.76 (s, 6H); 2.57 (s, 6H); 3.42 (s, 2H); 3.61 (s, 2H); 4.25 (q, 4H, J = 7.1 Hz); 6.60 (s, 1H); 6.61 (d, 1H, J = 8.1 Hz); 6.76 (d, 1H, J = 8.1 Hz). HRMS (EI$^+$): calcd for M$^+$, 450.2267; found, 450.2266.

Synthesis of 8-(3,4-Diaminophenyl)-2,6-diethyl-4,4-difluoro-1,3,5,7-tetramethyl-4-bora-3a,4a-diaza-*s*-indacene (DAMBO-Et) and 8-(3,4-Diaminophenyl)-2,6-diethoxycarbonyl-4,4-difluoro-1,3,5,7-tetramethyl-4-bora-3a,4a-diaza-*s*-indacene (DAMBO-CO_2Et). DAMBO-Et and DAMBO-CO_2Et were prepared from **9a** and **9b** by the same method as that used to obtain **DAMBO**, in 43% and 44% yield, respectively.

DAMBO-Et. Recrystallized from $CHCl_3$/*n*-hexane to afford green crystals. ^{1}H NMR ($CDCl_3$): δ 0.98 (t, 6H, J = 7.5 Hz); 1.43 (s, 6H); 2.30 (q, 4H, J = 7.5 Hz); 2.51 (s, 6H); 3.46 (s, 2H); 3.52 (s, 2H); 6.57 (d, 1H, J = 8.4 Hz); 6.59 (s, 1H); 6.78 (d, 1H, J = 8.4 Hz). ^{13}C NMR ($CDCl_3$): δ 11.8, 12.5, 14.6, 17.1, 116.4, 117.0, 120.1, 127.3, 131.2, 132.4, 135.1, 135.3, 138.6, 141.1, 153.1. HRMS (EI$^+$): calcd for M$^+$, 410.2453; found, 410.2446. Mp: 280−283 °C (dec). Anal. Calcd for $C_{23}H_{29}BF_2N_4 \cdot 0.1CHCl_3$: C, 65.71; H, 6.95; N, 13.27. Found: C, 66.09; H, 6.65; N, 13.28.

DAMBO-CO_2Et. Recrystallized from $CHCl_3$/*n*-hexane to afford green crystals. ^{1}H NMR ($CDCl_3$): δ 1.33 (t, 6H, J = 7.1 Hz); 1.82 (s, 6H); 2.82 (s, 6H); 3.50 (s, 2H); 3.62 (s, 2H); 4.28 (q, 4H, J = 7.1 Hz); 6.55 (dd, 1H, J = 1.8, 8.3 Hz); 6.56 (d, 1H, J = 1.8 Hz); 6.82 (d, 1H, J = 8.3 Hz). ^{13}C NMR ($CDCl_3$): δ 14.0, 14.3, 14.9, 60.2, 115.7, 117.2, 119.6, 122.2, 125.6, 131.9, 135.8, 136.2, 147.0, 147.9, 158.9, 164.5. HRMS (EI$^+$): calcd for M$^+$, 498.2250; found, 498.2222. Mp: 241−242 °C. Anal. Calcd for $C_{25}H_{29}BF_2N_4O_4 \cdot 0.5H_2O$: C, 59.18; H, 5.96; N, 11.04. Found: C, 59.41; H, 5.75; N, 11.11.

Synthesis of 8-(5-Benzotriazolyl)-2,6-diethyl-4,4-difluoro-1,3,5,7-tetramethyl-4-bora-3a,4a-diaza-*s*-indacene (DAMBO-Et-T) and 8-(5-Benzotriazolyl)-2,6-diethoxycarbonyl-4,4-difluoro-1,3,5,7-tetramethyl-4-bora-3a,4a-diaza-*s*-indacene (DAMBO-CO_2Et-T). DAMBO-Et-T and DAMBO-CO_2Et-T were prepared from DAMBO-Et and DAMBO-CO_2Et by a method similar to that used for DAMBO-T, in 20% and 85% yield, respectively.

DAMBO-Et-T. Recrystallized from $CHCl_3$/*n*-hexane to afford brown needles. ^{1}H NMR ($CDCl_3$): δ 0.96 (t, 6H, J = 7.5 Hz); 1.17 (s, 6H); 2.28 (q, 4H, J = 7.5 Hz); 2.55 (s, 6H); 7.41 (d, 1H, J = 8.6 Hz); 7.86 (br, 1H); 8.07 (br, 1H); 12.93 (br, 1H). MS (EI): 421 (M$^+$). HRMS (EI$^+$): calcd for M$^+$, 421.2249; found, 421.2258. Mp: 206−207 °C. Anal. Calcd for $C_{23}H_{26}BF_2N_5$: C, 65.57; H, 6.22; N, 16.62. Found: C, 65.87; H, 6.41; N, 16.36.

DAMBO-CO_2Et-T. Recrystallized from $CHCl_3$/*n*-hexane to afford bright yellow needles. ^{1}H NMR ($CDCl_3$): δ 1.32 (t, 6H, J = 7.1 Hz); 1.55 (s, 6H); 2.86 (s, 6H); 4.28 (q, 4H, J = 7.1 Hz); 7.38 (dd, 1H, J = 1.1, 8.6 Hz); 7.88 (br, 1H); 8.10 (br, 1H). HRMS (EI$^+$): calcd for M$^+$, 509.2046; found, 509.2019. Mp: 229−230 °C. Anal. Calcd for $C_{25}H_{26}BF_2N_5O_4 \cdot H_2O$: C, 56.94; H, 5.35; N, 13.28. Found: C, 57.04; H, 5.19; N, 12.98.

Synthesis of 3-(2-Methoxycarbonylethyl)-2,4-dimethylpyrrole (10). Methyl 5-(benzyloxycarbonyl)-2,4-dimethyl-3-pyrrolepropionate (3.1 g, 9.8 mmol) was dissolved in 100 mL of acetone. After the addition of 10% Pd−C (50 mg), the mixture was stirred vigorously under a H_2 atmosphere overnight. The Pd−C was filtered off and washed with acetone. The residue after evaporation of the filtrate was dissolved in 10 mL of TFA and stirred at 40 °C for 10 min under an Ar atmosphere. $CHCl_3$ was added to the reaction mixture, and this was washed with water. The aqueous solution was back-extracted with $CHCl_3$, and the combined organic extracts were washed with aqueous sodium carbonate and water, dried over $MgSO_4$, filtered, and evaporated. The crude compound was purified by column chromatography over silica gel (CH_2Cl_2) to afford a yellow oil (1.6 g, yield 90%). ^{1}H NMR ($CDCl_3$): δ 2.03 (d, 3H, J = 0.9 Hz); 2.18 (s, 3H); 2.45 (m, 2H); 2.72 (m, 2H); 3.67 (s, 3H); 6.38 (d, 1H, J = 0.9 Hz); 7.53 (s, 1H). MS (EI): 181 (M$^+$).

Synthesis of 6-(4-Amino-3-nitrophenyl)-4,4′-bis-(2-methoxycarbonylethyl)-3,3′,5,5′-tetramethylpyrromethene (11). 11 was prepared from **7** and **10** by the same method as that used to obtain **8a**, in 76% yield. ^{1}H NMR ($CDCl_3$): δ 1.37 (s, 6H); 2.33 (s, 6H); 2.36 (t, 4H, J = 7.1, 8.4 Hz); 2.63 (t, 4H, J = J = 7.1, 8.4 Hz); 3.65 (s, 6H); 6.32 (s, 2H); 6.92 (d, 1H, J = 8.6 Hz); 7.26 (dd, 1H, J = 2.0, 8.6 Hz); 8.06 (d, 1H, J = 2.0 Hz). HRMS (EI$^+$): calcd for M$^+$, 508.2323; found, 508.2327.

Synthesis of 8-(4-Amino-3-nitrophenyl)-4,4-difluoro-2,6-bis-(2-methoxycarbonylethyl)-1,3,5,7-tetramethyl-4-bora-3a,4a-diaza-*s*-indacene (12). 12 was prepared from **11** by the same method as that used to obtain **DAMBO**, in 31% yield. ^{1}H NMR ($CDCl_3$): δ 1.46 (s, 6H); 2.37 (t, 4H, J = 7.3, 8.3 Hz); 2.54 (s, 6H); 2.65 (t, 4H, J = 7.3, 8.3 Hz); 3.66 (s, 6H); 6.32 (s, 2H); 6.99 (d, 1H, J = 8.4 Hz); 7.24 (dd, 1H, J = 1.8, 8.4 Hz); 8.06 (d, 1H, J = 1.8 Hz). HRMS (EI$^+$): calcd for M$^+$, 556.2305; found, 556.2294.

Synthesis of 8-(4-Amino-3-nitrophenyl)-2,6-bis-(2-carboxyethyl)-4,4-difluoro-1,3,5,7-tetramethyl-4-bora-3a,4a-diaza-*s*-indacene (13). 12 (183 mg, 0.33 mmol) was dissolved in 100 mL of MeOH, then 10 mL of 0.2 N NaOH was added, and the mixture was refluxed at 80 °C for 1 h. The reaction mixture was evaporated and acidified with 2 N HCl. The aqueous solution was extracted with ethyl acetate. The combined organic extracts were dried over Na_2SO_4, filtered, and evaporated. The crude compound was purified by column chromatography over silica gel (CH_2Cl_2/ MeOH, 10:1) to afford an orange powder (87 mg, yield 50%). ^{1}H NMR (CD_3OD): δ 1.44 (s, 6H); 2.26 (t, 4H, J = 7.3, 7.9 Hz); 2.40 (s, 6H); 2.57 (t, 4H, J = 7.3, 7.9 Hz); 7.07 (d, 1H, J = 8.6 Hz); 7.17 (dd, 1H, J = 2.0, 8.6 Hz); 7.88 (d, 1H, J = 2.0 Hz). HRMS (ESI$^+$): calcd for [M+Na]$^+$, 551.1889; found, 551.1922.

Synthesis of 8-(3,4-Diaminophenyl)-2,6-bis(2-carboxyethyl)-4,4-difluoro-1,3,5,7-tetramethyl-4-bora-3a,4a-diaza-*s*-indacene (DAMBO-P^H). 13 (87 mg, 0.16 mmol) was dissolved in 100 mL of MeOH. After the addition of 10% Pd−C (50 mg), the mixture was stirred vigorously under a H_2 atmosphere. When TLC monitoring (silica; CH_2Cl_2/ MeOH, 5:1) showed complete consumption of **13**, the Pd−C was filtered off and washed with MeOH. The residue after evaporation of the filtrate was purified by column chromatography over silica gel (CH_3CN/H_2O, 10:1) and recrystallized from EtOH to afford orange needles (32 mg, yield 38%). ^{1}H NMR (CD_3OD): δ 1.51 (s, 6H); 2.28 (t, 4H, J = 7.1, 8.4 Hz); 2.47 (s, 6H); 2.64 (t, 4H, J = 7.1, 8.4 Hz); 6.46 (dd, 1H, J =

2.0, 7.9 Hz); 6.59 (d, 1H, J = 2.0 Hz); 6.83 (d, 1H, J = 7.9 Hz). ^{13}C NMR (CD_3OD): δ 12.3, 12.6, 20.7, 36.2, 116.9, 117.6, 119.9, 127.0, 130.5, 132.6, 137.1, 137.1, 140.9, 144.2, 154.3, 177.7. HRMS (ESI$^+$): calcd for $[M+Na]^+$, 521.2148; found, 521.2127. Mp: >300 °C. Anal. Calcd for $C_{25}H_{29}BF_2N_4O_4$: C, 60.25; H, 5.87; N, 11.24. Found: C, 60.31; H, 5.86; N, 11.42.

Synthesis of 8-(5-Benzotriazolyl)-2,6-bis(2-carboxyethyl)-4,4-difluoro-1,3,5,7-tetramethyl-4-bora-3a,4a-diaza-*s*-indacene (DAMBO-P^H-T). DAMBO-P^H-T was prepared from DAMBO-P^H by a method similar to that used for DAMBO-T. The resulting mixture was extracted with ethyl acetate. The combined organic extracts were dried over Na_2SO_4, filtered, and evaporated. The crude compound was purified by column chromatography over silica gel (CH_3CN/H_2O, 10:1) and recrystallized from EtOH to afford brown crystals (yield 82%). ^{1}H NMR (CD_3OD): δ 1.24 (s, 6H); 2.30 (t, 4H, J = 7.1, 8.3 Hz); 2.51 (s, 6H); 2.63 (t, 4H, J = 7.1, 8.3 Hz); 7.43 (d, 1H, J = 8.4 Hz); 7.89 (s, 1H); 8.08 (d, 1H, J = 8.4 Hz). HRMS (ESI$^+$): calcd for $[M+Na]^+$, 532.1944; found, 532.1927. Mp: 235−240 °C dec

Fluorometric Analysis. The slit width was 2.5 nm for both excitation and emission. The photon multiplier voltage was 700 V. Relative quantum efficiencies of fluorescence of BODIPY derivatives were obtained by comparing the area under the corrected emission spectrum of the test sample excited at 492 nm in 0.1 N NaOH with that of a solution of fluorescein, which has a quantum efficiency of 0.85 according to the literature.[23]

In the experiment to measure the pH profile of fluorescence and the time course of fluorescence increase, the slit width was 5.0 nm for excitation and 2.5 nm for emission and the photon multiplier voltage was 750 V. Compounds were dissolved in DMSO to make a 5 mM stock solution, which was diluted to the required concentration for measurement.

Computational Methods. All structures were computed using hybrid density functional theory (B3LYP)[24] with the 6-31G* basis set as implemented in Gaussian 98W.[25] Several starting geometries were used for the geometry optimization to ensure that the optimized structure corresponds to a global minimum.

(23) Paeker, A.; Rees, W. T. *Analyst* **1960**, *85*, 587−600.

HPLC Analysis. HPLC analyses were performed on an Inertsil ODS-3 (4.6 × 250 mm) column using an HPLC system composed of a pump (PU-980, Jasco) and a detector (UV-970 or FP-920, Jasco).

Cyclic Voltammetry. Cyclic voltammetry was performed on a 600A electrochemical analyzer (ALS). A three-electrode arrangement in a single cell was used for the measurements: a Pt wire as the auxiliary electrode, a Pt electrode (i.d. = 1.6 mm) as the working electrode, and a Ag/Ag^+ electrode as the reference electrode. The sample solutions contained 1.0×10^{-3} M sample and 0.1 M tetrabutylammonium perchlorate (TBAP) as a supporting electrolyte in acetonitrile, and argon was bubbled for 10 min before each measurement. The scan rate was 0.1 V s^{-1}. Obtained potentials (vs Ag/Ag^+) were converted to those vs a saturated calomel electrode (SCE) by adding 0.25 V.

Acknowledgment. This work was supported in part by the Ministry of Education, Science, Sports and Culture of Japan (grants 11794026, 12470475, and 12557217 to T.N., 12771349, 13557209, and 14030023 to Y.U.), by the Research Foundation for Opt-Science and Technology, by the Kowa Life Science Foundation, and by the Advanced and Innovational Research program in Life Sciences from the Ministry of Education, Culture, Sports, Science and Technology, the Japanese Government.

JA037944J

(24) (a) Becke, A. D. *J. Chem. Phys.* **1993**, *98*, 1372−1377. (b) Becke, A. D. *J. Chem. Phys.* **1993**, *98*, 5648−5652. (c) Lee, C.; Yang, W.; Parr, R. G. *Phys. Rev. B* **1988**, *37*, 785−789.

(25) Frisch, M. J.; Trucks, G. W.; Schlegel, H. B.; Scuseria, G. E.; Robb, M. A.; Cheeseman, J. R.; Zakrzewski, V. G.; Montgomery, J. A., Jr.; Stratmann, R. E.; Burant, J. C.; Dapprich, S.; Millam, J. M.; Daniels, A. D.; Kudin, K. N.; Strain, M. C.; Farkas, O.; Tomasi, J.; Barone, V.; Cossi, M.; Cammi, R.; Mennucci, B.; Pomelli, C.; Adamo, C.; Clifford, S.; Ochterski, J.; Petersson, G. A.; Ayala, P. Y.; Cui, Q.; Morokuma, K.; Malick, D. K.; Rabuck, A. D.; Raghavachari, K.; Foresman, J. B.; Cioslowski, J.; Ortiz, J. V.; Stefanov, B. B.; Liu, G.; Liashenko, A.; Piskorz, P.; Komaromi, I. R.; Gomperts, R.; Martin, L.; Fox, D. J.; Keith, T.; Al-Laham, M. A.; Peng, C. Y.; Nanayakkara, A.; Gonzalez, C.; Challacombe, M. P.; Gill, M. W.; Johnson, B.; Chen, W.; Wong, M. W.; Andres, J. L.; Gonzalez, C.; Head-Gordon, M.; Replogle, E. S.; Pople, J. A. *Gaussian 98*, revision A.6; Gaussian, Inc.: Pittsburgh, PA, 1998.

J|A|C|S
ARTICLES
Published on Web 10/12/2004

Rational Principles for Modulating Fluorescence Properties of Fluorescein

Tasuku Ueno,[†] Yasuteru Urano,[†,‡] Ken-ichi Setsukinai,[†] Hideo Takakusa,[†] Hirotatsu Kojima,[†] Kazuya Kikuchi,[†,‡] Kei Ohkubo,[§] Shunichi Fukuzumi,[§] and Tetsuo Nagano*[,†]

Contribution from the Graduate School of Pharmaceutical Sciences, The University of Tokyo, Hongo, Bunkyo-ku, Tokyo 113-0033, Japan, Presto, JST Agency, 4-8-1 Honcho, Kawaguchi, Saitama, 332-0012, Japan, and Graduate School of Engineering, Osaka University, CREST, JST Agency, Yamada-oka, Suita, Osaka 565-0871, Japan

Received March 27, 2004; E-mail: tlong@mol.f.u-tokyo.ac.jp

Abstract: Rational design strategies based on practical fluorescence modulation mechanisms would enable us to rapidly develop novel fluorescence probes for target molecules. Here, we present a practical and general principle for modulating the fluorescence properties of fluorescein. We hypothesized that (a) the fluorescein molecule can be divided into two moieties, i.e., the xanthene moiety as a fluorophore and the benzene moiety as a fluorescence-controlling moiety, even though there is no obvious linker structure between them, and (b) the fluorescence properties can be modulated via a photoinduced electron transfer (PeT) process from the excited fluorophore to a reducible benzene moiety (donor-excited PeT; d-PeT). To evaluate the relationship between the reduction potential of the benzene moiety and the fluorescence properties, we designed and synthesized various derivatives in which the reduction potential of the benzene moiety was fine tuned by introducing electron-withdrawing groups onto the benzene moiety. Our results clearly show that the fluorescence properties of fluorescein derivatives were indeed finely modulated depending upon the reduction potential of the benzene moiety. This information provides a basis for a practical strategy for rational design of novel functional fluorescence probes.

Introduction

Fluorescence probes are excellent tools to analyze and clarify the roles of biomolecules in living cells.[1] Many fluorescence probes for detecting biomolecules have been developed,[2−7] though most of them were obtained not rationally but empirically. Novel rational approaches are required for efficient development of practical fluorescence probes. An important but imperfectly realized goal is to establish a general strategy to create a wide variety of practical fluorescence probes for certain biomolecules. Recent efforts in our laboratory have been focused on establishment of the rational designing principles for functional fluorescence probes.

Fluorescein is widely employed as a platform for various fluorescence probes and fluorescence labels because of its high fluorescence quantum efficiency (Φ_{fl}) in aqueous media.[1,4−7] Recently, we found that the fluorescein molecule could be understood as a directly linked donor−acceptor system (Figure 1A). The two parts are conjugatively uncoupled since they are orthogonal to each other, and their fluorescence properties can be modulated by intramolecular photoinduced electron transfer (PeT) from the benzene moiety to the acceptor fluorophore (acceptor-excited PeT; a-PeT).[8,9] These findings enabled us to design flexibly many kinds of functional fluorescence probes based on the change of the oxidation potential of the benzene moiety upon encountering a target molecule, such as DMAX for singlet oxygen.[8] In this way, establishment of a rational design strategy made it possible to develop novel fluorescence probes for target molecules with high efficiency.[6−8,10]

Here we report a novel principle for controlling the fluorescence properties of the fluorescein molecule based on electron

[†] The University of Tokyo.
[‡] Presto, JST Agency.
[§] Osaka University, CREST, JST Agency.

(1) Bissell, R. A.; de Silva, A. P.; Gunarathe, H. Q. N.; Lynch, P. L. M.; McCoy, C. P.; Maguire, G. E. M.; Sandanayake, K. R. A. S. In *Fluorescent Chemosensors for Ion and Molecule Recognition*; Czarnik, A. W., Ed.; ACS Symposium Series 538; American Chemical Society: Washington, D.C., 1993; Chapter 9.
(2) Grynkiwicz, G.; Poenie, M.; Tsien, R. Y. *J. Biol. Chem.* **1985**, *260*, 3440−50.
(3) Minta, A.; Kao, J. P. Y.; Tsien, R. Y. *J. Biol. Chem.* **1989**, *264*, 8171−8178.
(4) James, T. D.; Sandanayake, K. R. A. S.; Shinkai, S. *Angew. Chem., Int. Ed.* **1994**, *33*, 2207−2209.
(5) Walkup, G. K.; Burdette, S. C.; Lippard, S. J.; Tsien, R. Y. *J. Am. Chem. Soc.* **2000**, *122*, 5644−5645.
(6) Hirano, T.; Kikuchi, K.; Urano, Y.; Higuchi, T.; Nagano, T. *J. Am. Chem. Soc.* **2000**, *122*, 12399−12400.
(7) Setsukinai, S.; Urano, Y.; Kakinuma, K.; Majima, H. J.; Nagano, T. *J. Biol. Chem.* **2003**, *278*, 3170−3175.
(8) Tanaka, K.; Miura, T.; Umezawa, N.; Urano, Y.; Kikuchi, K.; Higuchi, T.; Nagano, T. *J. Am. Chem. Soc.* **2001**, *123*, 2530−2536.
(9) Miura, T.; Urano, Y.; Tanaka, K.; Nagano, T.; Ohkubo, K.; Fukuzumi, S. *J. Am. Chem. Soc.* **2003**, *125*, 8666−8671.
(10) Umezawa, N.; Tanaka, K.; Urano, Y.; Kikuchi, K.; Higuchi, T.; Nagano, T. *Angew. Chem., Int. Ed.* **1999**, *38*, 2899−2901.

10.1021/ja048241k CCC: $27.50

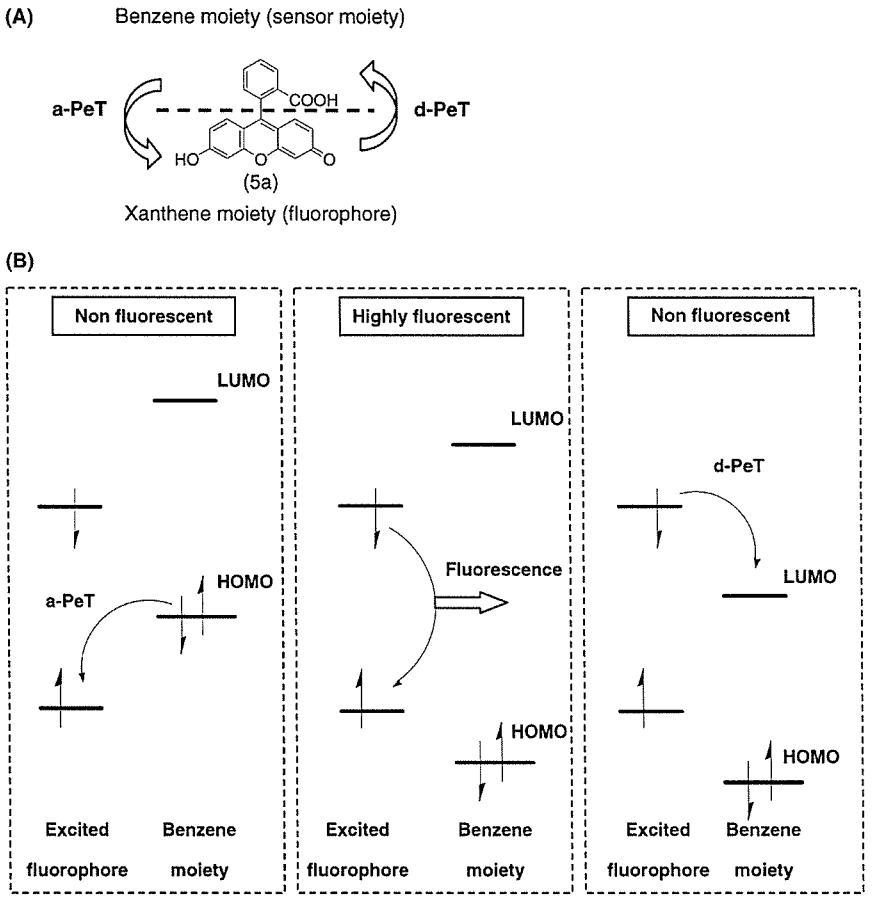

Figure 1. (A) Fluorescein (**5a**) was divided into two parts, the benzene moiety and xanthene moiety. (B) Schematic molecular orbital diagram of the fluorescence off/on switch including the PeT process.

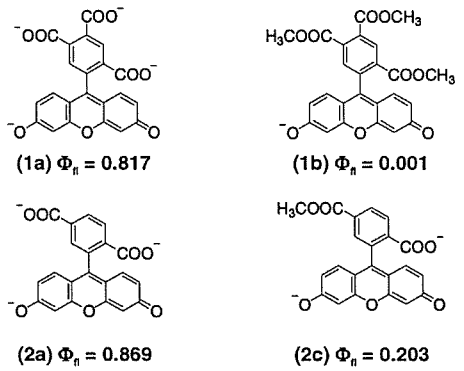

Figure 2. Structures and fluorescence properties of carboxyfluorescein derivatives (**1a**, **1b**, **2a**, **2c**) measured in phosphate buffer pH 9.

transfer from the excited fluorophore to the benzene moiety (donor-excited PeT; d-PeT), i.e., the opposite direction to a-PeT (Figure 1A). These findings have allowed us to construct another widely applicable strategy for rational design of a novel class of functional fluorescence probes. The validity of this approach was confirmed by applying it to develop a novel fluorescence probe for reactive peroxometal species with an unique pattern of sensitivity.

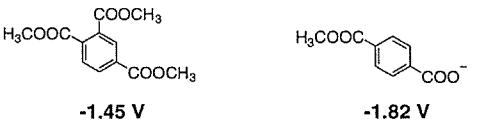

Figure 3. Electrochemical properties of the benzene moiety of carboxyfluorescein derivatives (**1b**, **2c**) in aqueous media (V vs SCE).

Results and Discussion

Fluorescence Quenching by the Electron-Deficient Benzene Moiety. We recently designed and synthesized dicarboxyfluorescein (**1a**) and its trimethyl ester derivative (**1b**) mainly in order to obtain probes with improbed water solubility. Owing to the presence of electron-withdrawing groups, the electron densities of the benzene moieties were lowered. According to our previous studies,[8,9] the oxidation potential of the benzene moiety is the most important factor determining the Φ_{fl} value of fluorescein. Therefore, we considered that **1a** and **1b** should be highly fluorescent (Figure 2). As anticipated, **1a** was highly fluorescent (Φ_{fl} = 0.817), but unexpectedly, the fluorescence of **1b** was significantly quenched (Φ_{fl} = 0.001). A similar phenomenon was also observed in the 6-carboxyfluorescein derivative (**2a**, **2c**). From the viewpoint of a-PeT, there are some apparent contradictions in these results.

To understand the mechanism underlying the fluorescence quenching further, we focused particularly on the reduction

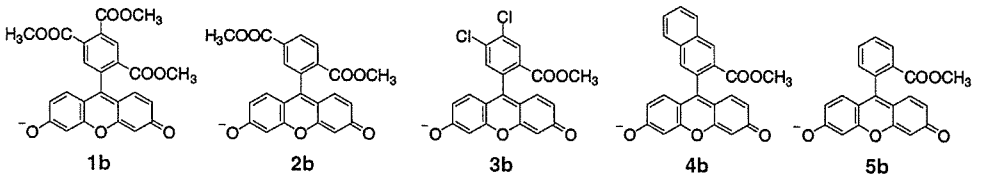

Figure 4. Structures of benzene-moiety-substituted fluorescein derivative (**1b**–**5b**).

Table 1. Photochemical Properties of Benzene-Moiety-Substituted Fluorescein Derivatives (**1b**–**5b**)

	reduction potential of benzene moiety (V vs SCE)[a]	absorption maximum (nm)[b]	emission maximum (nm)[b]	Φ_{fl}[b-d]	fluorescence lifetime[b] (ns)
1b	−1.65	501	525	0.001	n.d.[e]
2b	−1.79	498	524	0.009	0.56
3b	−1.84	499	527	0.213	2.55
4b	−2.11	495	517	0.673	3.58
5b	−2.36	494	518	0.761	3.93

[a] Measured in acetonitrile. [b] Measured in 0.1 M phosphate buffer (pH 9). [c] Excited at 490 nm. [d] Calculated by using fluorescein as a fluorescence standard (Φ_{fl} = 0.850). [e] Below the detection limit.

potential of the benzene moiety. Our working hypothesis is that the fluorescence properties of fluorescein derivatives are influenced by not only the oxidation potential of the benzene moiety, but also the reduction potential of the benzene moiety. In principle, PeT is able to take place in both directions,[11–14] from the excited fluorophore to the lowest unoccupied molecular orbital (LUMO) of an electron acceptor (donor-excited PeT; d-PeT) as well as in the opposite direction, i.e., a-PeT (Figure 1B). If the reduction potential of the electron acceptor is high enough for electron transfer to occur thermodynamically, singlet excited energy will be lost as a consequence of electron transfer and the fluorophore will be in the off state. By taking advantage of the intramolecular donor–acceptor system, the fluorescein molecule might become useful as a platform not only for a-PeT probes, but also for d-PeT probes. To verify our hypothesis, we determined the reduction potential of the benzene moiety. The benzene moiety of **1b** has a 370 mV more positive reduction potential than that of **2c** in aqueous media (Figure 3). Moreover, the reduction potentials of the benzene moieties of **1a** and **2a**, highly fluorescent compounds, were not above −2.0 V. These results are consistent with our hypothesis.

Relationship between the Reduction Potential of the Benzene Moiety and the Φ_{fl} Value. Further, to appreciate fully the relationship between the reduction potential of the benzene moiety and the Φ_{fl} value, we designed and synthesized various fluorescein derivatives in which the benzene moieties are substituted with several electron-deficient aromatic rings. Their structures, the absorbance and fluorescence properties, the reduction potentials of their benzene moieties, and the relative quantum efficiencies of fluorescence (Φ_{fl}) in basic aqueous media are summarized in Figure 4 and Table 1. The absorbance and emission maxima showed no significant change among these derivatives, and thus the ground-state interaction between the benzene moiety and the xanthene moiety was small in each derivative. On the other hand, the Φ_{fl} values varied greatly,

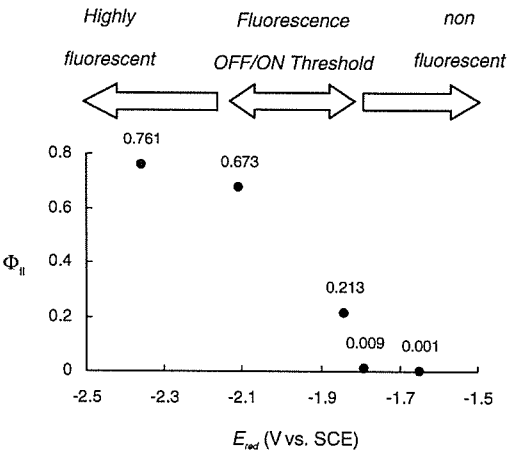

Figure 5. Relationship between the fluorescence quantum efficiency (Φ_{fl}) and the reduction potential (E_{red}).

depending on the reduction potential of the benzene moiety. In general, the feasibility of electron transfer between an excited-state sensitizer and quencher can be judged from the change in free energy (ΔG_{eT}). The ΔG_{eT} value could be calculated from the Rehm–Weller equation[15]

$$\Delta G_{eT} = E_{ox} - E_{red} - \Delta E_{0,0} - w_p$$

where E_{ox} and E_{red} are the oxidation and reduction potentials of electron donor and acceptor, $\Delta E_{0,0}$ is the singlet excited energy, and w_p is the work term for the charge separation state.[15] Owing to the similarity of their structures and the alteration in charge which accompanies electron transfer, fluorescein derivatives (**1b**–**5b**) have almost the same values of E_{ox}, $E_{0,0}$, and w_p. Therefore, in this study the E_{red} value plays a primary role in deciding the feasibility of electron transfer. Indeed, the Φ_{fl} values of **1b**–**5b** were strongly modulated by changes in the E_{red} value. In the case of derivatives in which the reduction potential of benzene moiety is more negative than −2.1 V (vs SCE), very high Φ_{fl} values were observed. For reduction potentials more positive than −2.1 V, the Φ_{fl} values dropped sharply, finally reaching $\Phi_{fl} \approx 0$ in the case of **1b**. From these results we determined that the threshold level between fluorescence off and on lies from around −1.80 to −2.15 V (Figure 5). Despite the widespread use of a-PeT as a fluorescence modulating principle of current PeT probes,[3–10,16–18] to our knowledge there are few functional fluorescence probes which

(11) Kavarnos, G. J.; Turro, J. N. *Chem. Rev.* **1986**, *86*, 401–449.
(12) Rehm, J. M.; McLendon, G. L.; Nagasawa, Y.; Yoshihara, K.; Moser, J.; Grätzel, M. *J. Phys. Chem.* **1996**, *100*, 9577–9578.
(13) Ghosh, H. N. *J. Phys. Chem. B* **1999**, *103*, 10382–10387.
(14) Zhang, H.; Zhou, Y.; Zhang, M.; Shen, T.; Li, Y.; Zhu, D. *J. Phys. Chem. B* **2002**, *106*, 9597–9603.
(15) Rehm, D.; Weller, A. *Isr. J. Chem.* **1970**, *8*, 259–271.
(16) de Silva, A. P.; Gunaratne, H. Q. N.; Gunnlaugsson, T.; Huxley, A. J. M.; McCoy, C. P.; Rademacher, J. T.; Rice, T. E. *Chem. Rev.* **1997**, *97*, 1515–1566.
(17) Kollmannsberger, M.; Rurack, K.; Resch-Genger, U.; Daub, J. *J. Phys. Chem. A* **1998**, *102*, 10211–10220.
(18) Chen, C.; Yeh. R.; Lawrence, D. S. *J. Am. Chem. Soc.* **2002**, *124*, 3840–3841.

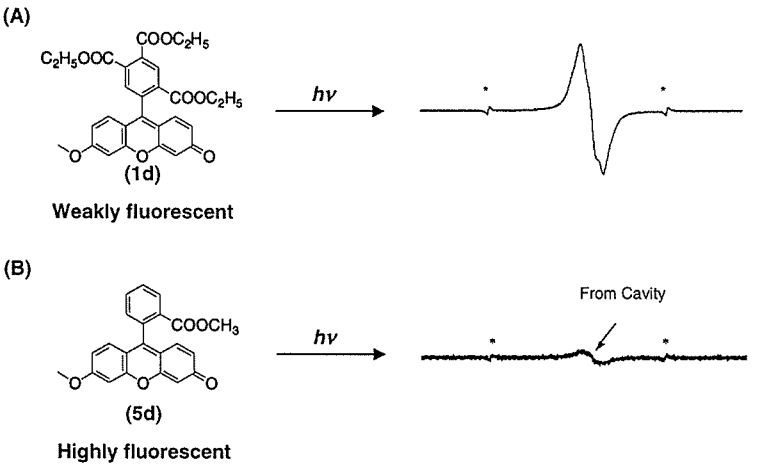

Figure 6. (A) Structure and ESR spectrum measured at 143 K of **1d** (1.0×10^{-3} M) under irradiation with light from a high-pressure mercury lamp in frozen acetonitrile. (B) Structure and ESR spectrum measured at 143 K of **5d** (1.0×10^{-3} M) under irradiation with light from a high-pressure mercury lamp in frozen acetonitrile. Asterisk denotes Mn^{2+} marker.

utilize the d-PeT concept. If such a d-PeT-based fluorescence modulation mechanism is applicable as a rational design principle for PeT probes, it would allow the development of novel and useful functional fluorescence probes for other kinds of biomolecules that could not be visualized with so-far developed a-PeT-based probes.

Direct Evidence that Fluorescence Quenching Is via Electron Transfer. To confirm the role of electron transfer, we tried to detect the production of radical species as a consequence of electron transfer in weakly fluorescent fluorescein derivatives. As previously reported by us, the formation of the radical ion pair state of a-PeT-based fluorescein derivatives under photoirradiation at 143 K could be observed with ESR. The ESR spectrum consisted of two characteristic signals of which one was attributable to the radical cation of the electron donor moiety and the other to the radical anion of the fluorophore.[9]

As expected, the weakly fluorescent fluorescein derivative **1d** exhibited strong ESR signals under photoirradiation at 143 K in acetonitrile (Figure 6A). Unfortunately, we could not assign this spectrum to two radical species due to signal broadening. However, the fact that no ESR signal could be observed under the same irradiation conditions with the strongly fluorescent fluorescein derivative **5d** led us to conclude that the d-PeT-based emission of weakly fluorescent fluorescein derivative was quenched via an electron transfer process.

Rational Design of a Novel Fluorescent Probe To Detect Reactive Oxygen Species. To confirm the potential of this principle, we then moved on to the development of a novel type of fluorescence probe, namely, MTM-CF, for reactive oxygen species.

MTM-CF contains a methylthiomethoxycarbonyl group, i.e., MTM ester, on the benzene moiety. MTM group is a protective group for the carboxyl group and can be easily removed with oxidizing agents.[19,20] A scheme showing reaction of MTM-CF with ROS is given in Figure 7. As expected, the fluorescence of MTM-CF was strongly extinguished but was

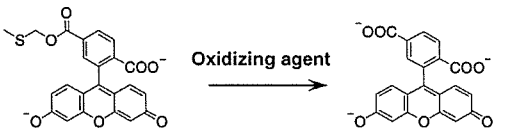

Abs/Em = 495/518, Φ_{fl} = 0.097 Abs/Em = 492/514, Φ_{fl} = 0.869

Figure 7. Reaction of MTM-CF with ROS. The fluorescence of MTM-CF was extinguished before reaction, and then oxidation of the MTM group by an oxidizing agent triggers elimination of the carboxyl group, yielding a highly fluorescent compound (**2a**).

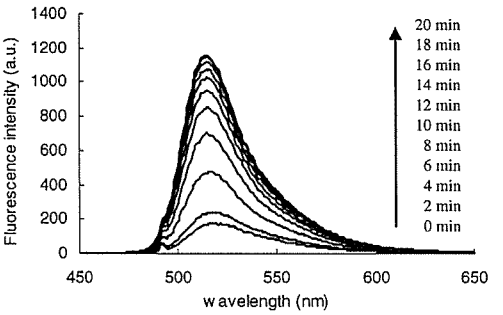

Figure 8. Emission spectra (excited at 490 nm) of MTM-CF (1 μM, 0.1% DMF) in 0.1 M sodium phosphate buffer (pH 7.4) 0, 2, 4, 6, 8, 10, 12, 14, 16, 18, and 20 min after reaction with a mixture of H_2O_2 and molybdate, permolybdate.

dramatically enhanced by adding a mixture of H_2O_2 and MoO_4^{2-}, permolybdate (Figure 8). Combination of transition metal and H_2O_2 was reported to generate potent oxidizing agents, namely, peroxometal species.[21-27]

(19) Wade, L. G.; Gerdes, J. M.; Wirth, R. P. *Tetrahedron Lett.* **1978**, *19*, 731–732.
(20) Gerdes, J. M.; Wade, L. G. *Tetrahedron Lett.* **1979**, *20*, 689–690.
(21) Connor, J. A.; Ebsworth, E. A. V. *Adv. Inorg. Chem. Radiochem.* **1964**, *6*, 279 and references therein.
(22) Aubry, J. M.; Cazin, B.; Duprat, F. *J. Org. Chem.* **1989**, *54*, 726–728.
(23) Mishinchi, S.; Matić, G.; Hutchison, K. A.; Pratt, W. B. *J. Biol. Chem.* **1990**, *265*, 11643–11649.
(24) Li, J.; Elberg, G.; Gefel, D.; Shechter, Y. *Biochemistry* **1995**, *34*, 6218–6225.
(25) Haque, S. J.; Flati, V.; Deb, A.; Williams, B. R. G. *J. Biol. Chem.* **1995**, *270*, 25709–25714.
(26) Mikalsen, S. V.; Kaalhus, O. *J. Biol. Chem.* **1998**, *273*, 10037–10045.
(27) Yamamoto, T.; Matsuzaki, H.; Konishi, H.; Ono, Y.; Kikkawa, U. *Biochem. Biophys. Res. Commun.* **2000**, *273*, 960–966.

Table 2. Fluorescence Increase of MTM-CF after Reaction with Several ROS[a]

reactant	MTM-CF	APF
permolybdate[b]	302	94
•OH[c]	<1	201
ClO^- [d]	<1	1000
blank	1	<1

[a] MTM-CF or APF (final 1.0×10^{-6} M, 0.1% DMF) was added to 0.1 M sodium phosphate buffer (pH 7.4). The fluorescence intensity was determined at 516 nm. [b] Na_2MoO_4 (1.0×10^{-2} M) and H_2O_2 (5.0×10^{-1} M) were added, and stirred for 3 min. [c] Ferrous perchlorate (1.0×10^{-4} M) and H_2O_2 (1.0×10^{-3} M) were added and stirred for 3 min. [d] ClO^- (1.0×10^{-6} M) was added and stirred for 3 min.

The Φ_{fl} value of MTM-CF was lower than that of **2c**, although both derivatives have one carbonate ester group in the same position. This observation can be explained thermodynamically in terms of the d-PeT process. Compared with the methyl ester, MTM ester is more potently electron-withdrawing. As a consequence, the benzene moiety of MTM-CF should have a more positive reduction potential than that of **2c**, and thus, MTM-CF would be quenched more efficiently via the d-PeT process.

MTM-CF is potentially useful as a tool to study the role of peroxometal species in many biological and chemical applications. While APF, one of the a-PeT-based ROS probes,[7] reacts with several highly reactive oxygen species, including permolybdate, MTM-CF has an unique sensitivity pattern to ROS owing to the moderate reactivity of the MTM group (Table 2). The difference in reactivity between these probes can be mainly ascribed to the distinct properties of the sensor moiety. In the case of a-PeT-based fluorescence probes, a highly oxidizable moiety is essential for modulating fluorescence, so target molecule recognition is limited to species that can interact with the highly oxidizable sensor. By contrast, a highly oxidizable moiety is not needed for d-PeT-based fluorescence probes. Therefore, a d-PeT-based design strategy should allow us to develop novel types of probes with a characteristic reactivity pattern which is different from those of currently known PeT probes.

The basic principle for modulating the fluorescence of MTM-CF is the change of reduction potential which is caused by conversion of the carbonyl group. In short, the key feature for modulating fluorescence is not the MTM group but the carbonyl group. Therefore, we can easily obtain probes with altered sensitivity and selectivity by converting the MTM group into another protecting group. This principle is not limited to benzoate ester derivatives and could be extended to general electron acceptors. We believe that this design approach may serve as a core strategy to create a novel class of functional fluorescence probes, e.g., for esterases, peptidases, and oxidoreductases.

Conclusion

In conclusion, we report herein a novel type of fluorescence modulation mechanism, d-PeT, i.e., fluorescence quenching based on electron transfer from the xanthene moiety to the benzene moiety of fluorescein derivatives. The value of this principle was confirmed by using it to develop a novel type of fluorescence probe, MTM-CF, for ROS. On the basis of this designing strategy, it should be possible to develop a novel class of PeT probes for a wide range of targets by introducing an appropriate sensor moiety. Now, we can choose either an oxidizable sensor moiety or a reducible moiety as the sensor moiety, and alteration of the redox potential is available as a fluorescence modulation switch. Thus, the fluorescence properties of fluorescein can be controlled by either a-PeT or d-PeT process, and this information provides the basis for a practical strategy for rational design of functional fluorescence probes to flexibly detect various biological events.

Experimental Section

Materials and General Instruments. General chemicals were of the best grade available, supplied by Tokyo Chemical Industries, Wako Pure Chemical, or Aldrich Chemical Co., and used without further purification. Other chemicals used were dimethyl sulfoxide (DMSO, fluorometric grade, Dojindo), *N,N*-dimethylformamide (DMF, fluorometric grade, Dojindo), and tetrabutylammonium perchlorate (TBAP, electrochemical grade, Fluka). Acetonitrile, acetone, DMF, methanol, and ethanol were used after appropriate distillation or purification. NMR spectra were recorded on a JNM-LA300 (JEOL) instrument at 300 MHz for ^1H NMR and at 75 MHz for ^{13}C NMR. Mass spectra (MS) were measured with a JMS-DX300(JEOL) for EI and a JMS-T100LC AccuTOF(JEOL) for ESI. All experiments were carried out at 298 K unless otherwise specified.

Synthesis and Characterization of Fluorescein Derivatives (1a–5a). 9-[1-(2,5-Dicarboxy)phenyl]-6-hydroxy-3*H*-xanthen-3-one (2,5-diCOOHPh X, **2a**)[28] and 9-[2-(3-carboxy)naphthyl]-6-hydroxy-3*H*-xanthen-3-one (2-COOHNaph X, **4a**)[29] were prepared according to the literature. Fluorescein derivatives (**1a**, **3a**) were synthesized by means of the following procedure: to pyromellitic anhydride (**1a**) or 4,5-dichlorophthalic anhydride (**3a**) (1 equiv) was added to a solution of resorcinol (2 equiv) in methanesulfonic acid. The resulting mixture was heated under dry Ar at 85 °C for 20–36 h. The cooled mixture was poured onto ice, followed by filtration. The residue, containing the fluorescein derivative, was dried in vacuo to constant weight. The crude product was purified by silica gel chromatography.

9-[1-(2,4,5-Tricarboxy)phenyl]-6-hydroxy-3*H*-xanthen-3-one (2,4,5-triCOOHPh X, dicarboxyfluorescein, 1a). ^1H NMR (300 MHz, CD_3OD): δ 6.56 (dd, 2H, $J = 2.2$, 8.6 Hz); 6.64 (d, 2H, $J = 8.6$ Hz); 6.70 (d, 2H, $J = 2.2$ Hz); 7.44 (s, 1H); 8.37 (s, 1H). ^{13}C NMR (75 MHz, DMSO-d_6): δ 102.3, 108.5, 112.7, 123.7, 125.3, 127.5, 129.7, 133.7, 140.4, 151.8, 159.7, 167.0, 167.3, 167.8. HRMS (ESI^+): calcd for $M^+ + 1$, 421.0559; found, 421.0528.

9-[1-(4,5-Dichloro 2-carboxy)phenyl]-6-hydroxy-3*H*-xanthen-3-one (4,5-diCl 2-COOHPh X, 3a). ^1H NMR (300 MHz, DMSO-d_6): δ 6.55 (dd, 2H, $J = 2.4$, 8.6 Hz); 6.66 (d, 2H, $J = 2.4$ Hz); 6.68 (d, 2H, $J = 8.6$ Hz); 7.74 (s, 1H); 8.26 (s, 1H); 10.17 (s, 2H). ^{13}C NMR (75 Hz, DMSO-d_6): δ 83.3, 102.4, 108.6, 126.4, 126.6, 126.8, 129.3, 133.5, 138.7, 151.9, 159.9, 166.6. HRMS (ESI^+): calcd for $M^+ + 1$, 400.9983; found, 400.9961. Mp: 360 °C (dec). Anal. Calcd for $C_{20}H_{10}Cl_2O_5$: N, 0; C, 59.87; H, 2.51. Found: N, 0; C; 59.65; H, 2.70.

Synthesis of Fluorescein Methyl Ester Derivatives (1b–5b). Fluorescein was purchased from Tokyo Chemical Industries. 9-[1-(2,5-Dimethoxycarbonyl)phenyl]-6-hydroxy-3*H*-xanthen-3-one (2,5-diCOOMe-Ph X, 2b)[30] was prepared according to the literature. Fluorescein derivatives (**1b**, **3b–5b**) were synthesized by means of the following procedure: to a suspension of a fluorescein or fluorescein derivative (**1a**, **3a–5a**) in methanol was added a few drops of sulfuric acid. The reaction mixture was refluxed for 20 h; then it was poured onto ice and extracted with AcOEt. The organic layer was dried over anhydrous Na_2SO_4 and evaporated. The crude product was purified by silica gel

(28) Rossi, F. M.; Kao, J. P. Y. *Bioconjugate Chem.* **1997**, *8*, 495–497.
(29) Tanaka, K.; Miura, T.; Umezawa, N.; Urano, Y.; Kikuchi, K.; Higuchi, T.; Nagano, T. *J. Am. Chem. Soc.* **2001**, *123*, 2530–2536.
(30) Takakusa, H.; Kikuchi, K.; Urano, Y.; Kojima, H.; Nagano, T. *Chem.-Eur. J.* **2003**, *9*, 1479–1485.

chromatography. The product was recrystallized from methanol/CH_2Cl_2 to afford fluorescein methyl ester derivatives (**1b**, **3b**−**5b**).

9-[1-(2,4,5-Trimethoxycarbonyl)phenyl]-6-hydroxy-3*H*-xanthen-3-one (2,4,5-triCOOMePh X, 1b). ^{1}H NMR (300 MHz, $CDCl_3$): δ 3.66 (s, 3H); 3.91 (s, 3H); 3.99 (s, 3H); 6.67 (br, 4H); 6.93 (d, 2H, J = 9.3 Hz); 7.78 (s, 1H); 8.61 (s, 1H). ^{13}C NMR (75 Hz, $CDCl_3$ + CD_3OD): δ 53.3, 53.6, 78.6, 104.4, 115.5, 130.8, 131.6, 132.5, 133.4, 133.7, 136.6, 138.3, 164.9, 167.2, 167.4. HRMS (ESI$^+$): calcd for [M + Na]$^+$, 458.0848; found, 458.0819. Mp: 270 °C (dec). Anal. Calcd for $C_{25}H_{18}O_9 \cdot CH_3OH$: N, 0; C, 63.16; H, 4.48. Found: N, 0; C, 64.94; H, 3.92.

9-[1-(3,4-Dichloro-2-methoxycarbonyl)phenyl]-6-hydroxy-3*H*-xanthen-3-one (4.5-diCl 2-COOMePh X, 3b). ^{1}H NMR (300 MHz, DMSO-d_6): δ 3.59 (s, 3H); 6.52 (br, 4H); 6.90 (d, 2H, J = 9.4 Hz); 7.91 (s, 1H); 8.33 (s,1H); 11.07 (br, 1H). ^{13}C NMR (300 MHz, DMSO-d_6): δ 53.8, 104.6, 105.1, 108.1, 131.1, 131.5, 133.3, 134.3, 165.3. HRMS (ESI$^+$): calcd for M$^+$ + 1, 421.0559; found, 421.0528. Mp: 330 °C (dec). Anal. Calcd for $C_{21}H_{12}Cl_2O_5 \cdot 0.25H_2O$: N, 0; C, 60.09; H, 3.00. Found: N, 0; C, 60.21; H, 3.21.

9-[2-(3-Methoxycarbonyl)naphthyl]-6-hydroxy-3*H*-xanthen-3-one (2-COOMeNaph X, 4b). ^{1}H NMR (300 MHz, DMSO-d_6): δ 3.63 (s, 3H); 6.30 (br, 4H); 6.84 (m, 4H); 7.76 (m, 2H); 8.06 (m, 2H); 8.30 (m, 1H); 8.89 (s, 1H); 11.04 (br, 1H). HRMS (ESI$^+$): calcd for M$^+$ + 1, 397.107; found, 397.105. Mp: 325 °C (dec). Anal. Calcd for $C_{25}H_{18}O_6 \cdot 0.75H_2O$: N, 0; C, 73.25; H, 4.30. Found: N, 0; C, 73.43; H, 4.37.

9-[1-(2-Methoxycarbonyl)phenyl]-6-hydroxy-3*H*-xanthen-3-one-(2-COOMePh X, 5b). ^{1}H NMR (300 MHz, DMSO-d_6): δ 3.63 (s, 3H); 6.23−6.33 (br, 2H); 6.70−6.87 (m, 4H); 7.77 (m, 2H); 8.06 (m, 2H); 8.31 (m, 1H); 8.89 (s, 1H); 11.04 (br, 1H). ^{13}C NMR (75 MHz, DMSO-d_6 + CD_3OD): δ 52.6, 103.0, 103.9, 115.6, 129.8, 130.7, 131.0, 131.3, 131.5, 133.6, 134.9, 153.7, 166.1. HRMS (ESI$^+$): calcd for M$^+$ + 1, 347.0919; found, 347.0889. Mp: 285 °C (dec). Anal. Calcd for $C_{21}H_{14}O_5$: N, 0; C, 72.83; H, 4.07. Found: N, 0; C, 72.58; H, 4.33.

Synthesis of Compound 2c. 6-Carboxyfluorescein diacetate (6-CF-DA)[31] was prepared according to the literature. 6-CF-DA (50 mg, 0.11 mmol) was dissolved in DMF (5 mL); iodomethane (19 mg, 0.13 mmol) and cesium carbonate (43 mg, 0.13 mmol) were added. The mixture was stirred at room temperature for 2 h, water was added, and reaction mixture was extracted with AcOEt (3 × 30 mL). The organic layer was dried over anhydrous Na_2SO_4 and concentrated in vacuo. The crude product was dissolved in methanol (10 mL). To this solution sodium methoxide (47 mg, 0.87 mmol) was added. The mixture was stirred at 0 °C for 1 h, then poured into 1 N HCl (aq), and extracted with AcOEt (3 × 50 mL). The organic layer was dried over anhydrous Na_2SO_4 and evaporated. The crude product was purified by silica gel chromatography to afford **2c** (7 mg, yield 16%).

9-[1-(5-Methoxycarbonyl 2-carboxy)phenyl]-6-hydroxy-3*H*-xanthen-3-one (5-COOMe 2-COOHPh X, 2c). ^{1}H NMR (300 MHz, CD_3OD): δ 3.86 (s, 3H); 6.52 (dd, J = 2.2, 8.6 Hz, 2H); 6.56 (d, J = 8.6 Hz, 2H); 6.69 (d, J = 2.2 Hz, 2H); 7.75 (d, J = 1.3 Hz, 1H); 8.09 (d, J = 7.9 Hz, 1H); 8.30 (dd, J = 1.3, 7.9 Hz, 1H). ^{13}C NMR (75 MHz, CD_3OD): 53.1, 103.6, 110.8, 113.8, 126.3, 130.2, 132.0, 137.8, 154.1, 166.9, 170.3. HRMS (ESI$^+$): calcd for M$^+$ + 1, 391.0817; found, 391.0795. Anal. Calcd for $C_{22}H_{14}O_7 \cdot H_2O$: N, 0; C, 64.71; O, 3.95. Found: N, 0; C, 64.81; H, 3.85.

Synthesis and Characterization of 1d and 5d. 9-[1-(2-Methoxycarbonyl)phenyl]-6-methoxy-3*H*-xanthen-3-one (**5d**) was prepared according to the literature.[9] 9-[1-(2,4,5-Triethoxycarbonyl)phenyl]-6-hydroxy-3*H*-xanthen-3-one (**1d**) was prepared via the following procedure: to a suspension of **1a** (500 mg, 1.19 mmol) in ethanol (500 mL) was added a few drops of sulfuric acid. The reaction mixture was refluxed for 20 h and then concentrated in vacuo. The residue was poured onto ice, and the whole mixture was extracted with AcOEt. The organic layer was dried over Na_2SO_4 and concentrated in vacuo to afford a crude product. The crude product (100 mg) was dissolved in DMF (5 mL); then iodomethane (42 mg, 0.30 mmol) and cesium carbonate (97 mg, 0.3 mmol) were added. The mixture was stirred at room temperature for 12 h, water (50 mL) was added, and the reaction mixture was extracted with AcOEt (3 × 60 mL). The combined organic layers were dried over anhydrous Na_2SO_4 and concentrated in vacuo. The crude product was purified by silica gel chromatography to afford **1d** in 28% yield in two steps.

9-[1-(2,4,5-Triethoxycarbonyl)phenyl]-6-methoxy-3*H*-xanthen-3-one (1d). ^{1}H NMR (300 MHz, $CDCl_3$): δ 0.88 (t, 3H, J = 3.7 Hz); 1.37 (t, 3H, J = 3.7 Hz); 1.44 (t, 3H, J = 3.7 Hz); 3.93 (s, 3H, b); 4.09 (m, 2H); 4.09 (q, 2H, J = 3.7 Hz); 4.40 (q, 2H, J = 3.7); 6.45 (d, 1H, J = 0.9 Hz); 6.55 (dd, 1H, J = 1.1, 4.5 Hz); 6.81 (d, 1H, J = 4.5 Hz); 6.83 (d, 1H, J = 4.5 Hz); 6.96 (d, 1H, J = 1.1 Hz); 8.02 (s, 1H); 8.56 (s, 1H). ^{13}C NMR (75 MHz, $CDCl_3$): δ 13.5, 13.9, 14.0, 56.0, 62.0, 62.3, 62.4, 100.4, 105.9, 113.5, 114.1, 117.6, 128.5, 129.7, 130.2, 130.8, 131.6, 133.0, 135.6, 136.8, 147.7, 154.1, 158.5, 163.8, 164.3, 165.7, 165.9, 185.5. HRMS (ESI$^+$): calcd for [M + Na]$^+$, 541.1474; found, 543.1436. abs_{max} = 460, 483 nm. em_{max} = 527 nm. Φ_{fl} = 0.148.

Synthesis and Characterization of MTM-CF. 6-CF-DA (150 mg, 0.32 mmol) was dissolved in DMF (5 mL). To this solution, chloromethyl methyl thioether (81 mg, 0.86 mmol) and cesium carbonate (309 mg, 0.65 mmol) were added. The mixture was stirred for 6 h at room temperature, water was added, and the whole mixture was extracted with 3 × 50 mL of AcOEt. The organic layer was dried and concentrated in vacuo. The crude product was purified by silica gel chromatography to afford MTM-CF DA (49 mg, yield 30%). MTM-CF DA (10 mg, 0.02 mmol) was dissolved in 0.1 M sodium phosphate buffer (50 mL) (2% DMF cosolvent). To this solution porcine liver esterase (10 mg) was added. The mixture was incubated for 25 min at 25 °C. After the reaction, reaction mixture was diluted with 1 M HCl (aq, 50 mL) and whole mixture was extracted with AcOEt (3 × 50 mL). The organic layer was dried over anhydrous Na_2SO_4 and concentrated in vacuo. The crude product was purified by silica gel chromatography to afford MTM-CF (1.3 mg, yield 13%).

MTM-CF-DA. ^{1}H NMR (300 MHz, $CDCl_3$): δ 2.27 (s, 3H); 2,32 (s, 6H); 5.38 (s, 2H); 6.80 (d, 2H, J = 4.3 Hz); 6.84 (dd, 2H, J = 1.8, 4.3 Hz); 7.12 (d, 2H, J = 1.8 Hz); 7.83 (d, 1H, J = 1.3 Hz); 8.12 (d, 1H, J = 8.1 Hz); 8.33 (dd, 1H, J = 1.3, 8.1 Hz). ^{13}C NMR (75 Hz, $CDCl_3$): δ 15.7, 21.0, 69.9, 81.9, 110.4, 115.5, 117.8, 125.2, 125.3, 128.7, 129.7, 131.4, 136.2, 151.4, 152.1, 152.8, 164.4, 167.8, 168.6. HRMS (ESI$^+$): calcd for [M + Na]$^+$, 543.07257; found, 543.07687.

MTM-CF. ^{1}H NMR (CD_3OD): δ 2.29 (s, 3H); 5.38 (s, 2H); 6.53 (dd, 2H, J = 2.3, 8.6 Hz); 6.60 (d, 2H, J = 8.6 Hz); 6.70 (d, 2H, J = 2.3 Hz); 7.76 (d, 1H, J = 1.5 Hz); 8.11 (d, 1H, J = 7.9 Hz); 8.33 (dd, 1H, J = 1.5, 7.9 Hz). HRMS (ESI$^-$): calcd for [M − 1]$^-$, 435.05385; found, 435.05384.

Preparation of Benzene Moieties of Fluorescein Derivatives. All the benzene moieties of methylated fluorescein derivatives, i.e., substituted methyl benzoates, are commercially available except 3,4-dichlorobenzoic acid methyl ester.

3,4-Dichlorobenzoic Acid Methyl Ester. 3,4-Dichlorobenzoic acid (100 mg, 1.05 mmol) was dissolved in DMF (10 mL), and iodomethane (177 mg, 1.26 mmol) and cesium carbonate (408 mg, 1.26 mmol) were added. The mixture was stirred at room temperature for 12 h, water (50 mL) was added, and reaction mixture was extracted with AcOEt (3 × 60 mL). The organic layers were dried over anhydrous Na_2SO_4 and concentrated in vacuo. The crude product was purified by silica gel chromatography and recrystallized from methanol to afford 3,4-dichlorobenzoic acid methyl ester (145 mg, yield 68%). ^{1}H NMR (300 MHz, $CDCl_3$): 3.93 (s, 3H); 7.52 (d, J = 8.4 Hz, 1H); 7.86 (dd, J = 2.0, 8.4 Hz, 1H); 8.12 (d, J = 2.0 Hz, 1H). ^{13}C NMR (75 MHz, $CDCl_3$): 52.4, 128.5, 129.8, 130.4, 131.4, 132.8, 137.4, 165.0. HRMS

(31) Mattingly, P. G. *Bioconjugate Chem.* **1992**, *9*, 430−431.

(EI$^+$): calcd for M^+, 203.97448; found, 203.9767. Mp: 46.4−47.3 °C. Anal. Calcd for $C_8H_6Cl_2O_2$: N, 0; C, 46.86; H, 2.95. Found: N, 0; C, 46.66; H, 3.15.

Fluorescence Properties and Quantum Efficiency of Fluorescence. Steady-state fluorescence spectroscopic studies were performed on an F 4500 (Hitachi). UV−vis spectra were obtained on a UV-1650PC (Shimazu) with 0.1 M sodium phosphate buffer (pH 9) and 0.1 M NaOH. Each solution contained up to 0.2% (v/v) DMSO as a cosolvent. For determination of the quantum efficiency of fluorescence (Φ_{fl}), fluorescein in 0.1 M NaOH (Φ_{fl}) was used as a fluorescence standard. The quantum efficiencies of fluorescence were obtained with the following equation (F denotes fluorescence intensity at each wavelength and $\Sigma[F]$ was calculated by summation of fluorescence intensity)

$$\Phi_{fl}^{sample} = \Phi_{fl}^{standard} Abs^{standard} \Sigma[F^{sample}]/Abs^{sample} \Sigma[F^{standard}]$$

Fluorescence decay of samples was recorded with a C4780 system (Hamamatsu Photonics). The solution of samples was prepared to be 5.0×10^{-6} M in 0.1 M sodium phosphate buffer (pH 9) containing 0.1% DMSO as a cosolvent. It was excited with an N_2:Coumarin 102 pulse laser. The obtained data were appropriately deconvoluted and fitted to monoexponential decay curves to determine the fluorescence lifetime (τ) of samples.

Cyclic Voltammetry. Cyclic voltammetry was performed on a 600A electrochemical analyzer (ALS).

(a) In Aqueous Media. A three-electrode arrangement in a single cell was used for the measurement: a Pt wire as the auxiliary electrode, a GC electrode as the working electrode, and an Ag/AgCl electrode as the reference electrode. The sample solution contained 0.1 M sodium phosphate pH 9 as a supporting electrolyte, and argon was bubbled for 2 min before each measurement.

(b) In Acetonitrile. A three-electrode arrangement in a single cell was used for the measurement: a Pt wire as the auxiliary electrode, GC electrode as the working electrode, and an Ag/Ag^+ electrode as the reference electrode. The sample solution contained 0.1 M tetrabutylammonium perchlorate as a supporting electrolyte in acetonitrile, and argon was bubbled for 2 min before each measurement.

ESR Measurements. The ESR measurements of the photoexcited compound were carried out with a JES−RE1XE X-band spectrometer (JEOL) equipped with a variable-temperature apparatus to detect the transient radical species in a solution of sample (1.0×10^{-3}) M in frozen acetonitrile at 143 K under irradiation with light from a high-pressure mercury lamp (USH-1005D, Ushio). A quartz ESR tube containing a deaerated acetonitrile solution of sample was irradiated with the high-pressure Hg lamp through an aqueous filter.

Acknowledgment. This study was performed through the Advanced and Innovational Research program in Life Sciences from the Ministry of Education, Culture, Sports, Science and Technology, the Japanese Government to T.N., by research grants from the Ministry of Education, Culture, Sports, Science and Technology of Japan (Grant Nos. 16689002 and 16651106 to Y.U.), by Kowa Life Science Foundation to Y.U., and by a Grant-in-Aid from the Ministry of Education, Culture, Sports, Science and Technology, Japan (Grant No. 16205020 to S.F.).

JA048241K

A Novel Fluorescent Probe for Zinc Ion Based on Boron Dipyrromethene (BODIPY) Chromophore

Hitomi KOUTAKA,[a] Jun-ichi KOSUGE,[a] Noboru FUKASAKU,[a] Tomoya HIRANO,[b] Kazuya KIKUCHI,[b,c] Yasuteru URANO,[b] Hirotatsu KOJIMA,[b] and Tetsuo NAGANO*,[b]

[a] *Daiichi Pure Chemicals Co., Ltd.; 2117 Muramatsu, Tokai, Ibaraki 319–1182, Japan:* [b] *Graduate School of Pharmaceutical Sciences, the University of Tokyo; 7–3–1 Hongo, Bunkyo-ku, Tokyo 113–0033, Japan: and* [c] *Presto, JST Corporation; 4–8–1 Honcho, Kawaguchi, Saitama 332–0012, Japan.*
Received December 24, 2003; accepted February 25, 2004

ZnAB has the combined structure of *N,N*-bis(2-pyridylmethyl)ethylenediamine as a specific chelater for Zn^{2+} and 1,3,5,7-tetramethyl-8-phenyl-boron dipyrromethene as a fluorophore. Complexation of ZnAB with Zn^{2+} produces a remarkable enhancement of fluorescence intensity. ZnAB has the advantages of less sensitivity to solvent polarity and pH than fluorescein-based Zn^{2+} probes. Furthermore, it is not influenced by other cations, such as Na^+, K^+, Ca^{2+}, and Mg^{2+}, which exist at high concentrations under physiological conditions, even at 2.5 mM. The results show that ZnAB is a Zn^{2+} probe suitable for biological applications.

Key words zinc; fluorescence; boron dipyrromethene (BODIPY); photoinduced electron transfer; *N,N*-bis(2-pyridylmethyl)ethylenediamine

Zinc ion (Zn^{2+}) is found in every cell in the human body, and is the second most abundant heavy metal ion after iron. It is an essential component of many enzymes and transcription factors (*e.g.*, carbonic anhydrase, zinc finger proteins, *etc.*).[1] In addition to this protein-bound Zn^{2+}, chelatable Zn^{2+} is present, especially in the brain,[2] pancreas[3] and spermatozoa.[4] Certain neurons in the brain contain a relatively large pool of free Zn^{2+} sequestered in vesicles in their terminals. Such Zn^{2+} is released from nerve terminals by excitatory signals, and modulates the function of glutamate receptors. In the pancreas, Zn^{2+} is co-stored with insulin in secretary vesicles of pancreatic β-cells, and is released when insulin is secreted.[5] Zn^{2+} also suppresses apoptosis,[6] and induces the formation of β-amyloid,[7] which may be related to the etiology of Alzheimer's disease.

Although Zn^{2+} plays many physiologically important roles, the mechanisms involved are still poorly understood. Therefore, several chemical tools for measuring Zn^{2+} in living cells have been developed.[8—16] Fluorescent probes based on quinoline, fluorescein, other fluorophores or proteins, have been reported. Some of these probes can be used to monitor the change of Zn^{2+} concentration under physiological conditions, but they suffer from problems such as inadequate selectivity, insufficient sensitivity, and pH-sensitivity. We have already developed fluorescein-based probes, ZnAFs,[17,18] which have high selectivity and sensitivity, and ZnAF-Rs,[19] whose structure is based on benzofuran derivatives, and which enable ratiometric measurement. Here we report the design and synthesis of a new fluorescent probe for Zn^{2+} based on the BODIPY (boron dipyrromethene) chromophore. BODIPY has a high molar extinction coefficient and fluorescence quantum yield. Furthermore, it has the advantages of less sensitivity to solvent polarity and pH than fluorescein-based Zn^{2+} probes, and its structure can be modified to change its excitation and emission wavelengths.

Results and Discussion

Probe Design Based on Photoinduced Electron Transfer Our group has developed fluorescein-based probes for nitric oxide (DAFs),[20,21] for singlet oxygen (DPAXs, DMAXs),[22,23] and for Zn^{2+} (ZnAFs). As a basis for the design of these probes, we have utilized the photoinduced electron transfer (PeT) between the xanthene ring, which is an electron acceptor and fluorophore, and the benzoic acid moiety, which is an electron donor, and the probes exhibit fluorescence off/on switching that is dependent on the highest occupied molecular orbital (HOMO) level of the benzoic acid moiety. Amino- or oxygen-substituted BODIPYs have already been reported as pH or alkali metal and alkaline earth metal sensors.[24—27] However, BODIPY-based functional probes have not yet been developed for biological applications.

The fluorescence property of 1,3,5,7-tetramethyl-8-phenyl-BODIPY is thought to be controlled by electron transfer between the phenyl ring at the 8-position and 1,3,5,7-tetramethyl-8-phenyl-BODIPY (Chart 1a), because the dihedral angle between the benzene ring and BODIPY is almost 90° (Chart 1b), as in the case of fluorescein. The free energy change of the PeT process can be described by the Rehm–Weller equation,[28]

$$\Delta G_{PeT} = E_{1/2}(D^+/D) - E_{1/2}(A/A^-) - \Delta E_{00} - C$$

where $E_{1/2}(D^+/D)$ and $E_{1/2}(A/A^-)$ are the ground-state oxidation potential of the donor and the reduction potential of the acceptor, respectively, ΔE_{00} is the excitation energy, and C is the electrostatic interaction term. Since the reduction potential and the excitation energy of 1,3,5,7-tetramethyl-BODIPY (BODIPY 505/515; absorption maximum: 501 nm, reduction potential: -1.16 V *vs.* SCE) were nearly the same as those of fluorescein,[29] the threshold of fluorescence off/on in BODIPY was expected to be similar to that in fluorescein derivatives.

Thus, we designed ZnAB (Chart 2). *N,N*-Bis(2-pyridylmethyl)ethylenediamine, which is used as an acceptor for Zn^{2+} of ZnAFs, is directly attached to the benzene ring of 1,3,5,7-tetramethyl-8-phenyl-BODIPY. In the absence of metal cations, its fluorescence intensity should be weak because of fluorescence quenching by PeT, and the chelation of

* To whom correspondence should be addressed. e-mail: tlong@mol.f.u-tokyo.ac.jp

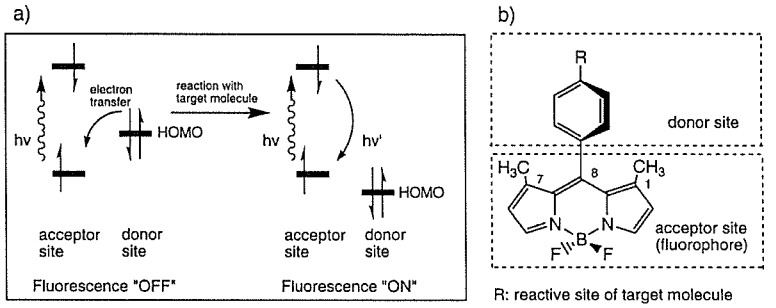

Chart 1. (a) Mechanism of Fluorescence OFF/ON Switching by Photoinduced Electron Transfer, (b) Design of Chemical Probe Based on Boron Dipyrromethene (BODIPY)

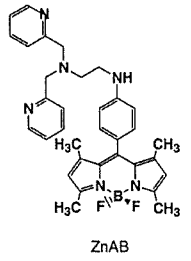

Chart 2. Chemical Structure of ZnAB

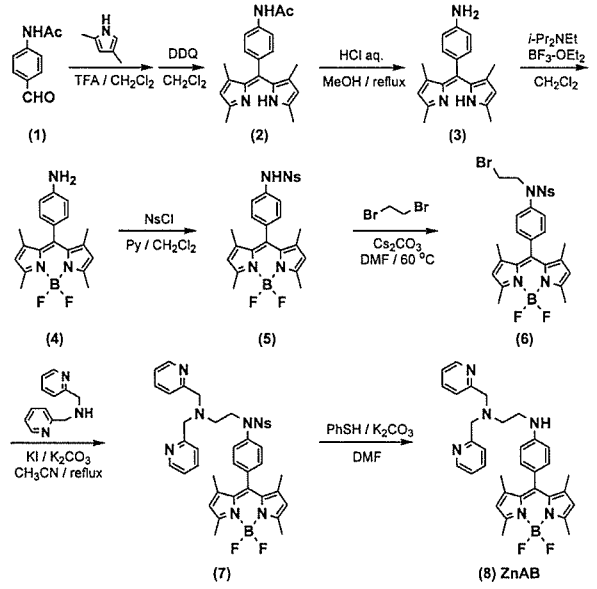

Chart 3. Synthetic Route to Compound (8): ZnAB

TFA: trifluoroacetic acid, Ns: 4-nitrobenzenesulfonyl, DDQ: 2,3-dichloro-5,6-dicyano-*p*-benzoquinone.

Zn^{2+} should induce a sufficient change of the HOMO level of the chelator-substituted benzene ring, so that the fluorescence intensity is increased because of the hindrance of PeT.

Synthesis of ZnAB The synthetic scheme for ZnAB is shown in Chart 3. Aminobodipy (**4**) was synthesized as previously reported,[30] and its amino group was protected with 4-nitrobenzensulfonyl group. Reaction with 1,2-dibromoethane, followed by 2,2′-dipycolylamine afforded compound

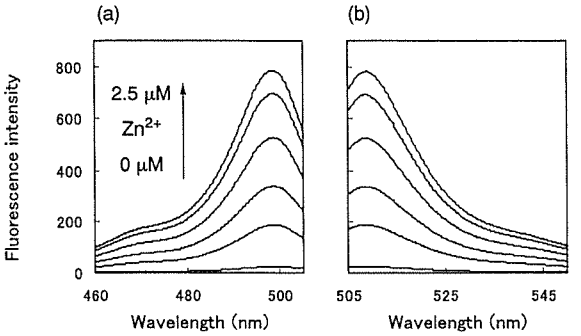

Fig. 1. (a) Excitation Spectra (Emission at 509 nm) and (b) Emission Spectra (Excitation at 499 nm) of ZnAB (2.5 μM) in the Presence of Various Concentrations of Zn^{2+} Ranging from 0 to 2.5 μM

These spectra were measured at pH 7.4 (CH_3CN : 100 mM HEPES buffer (I=0.1($NaNO_3$))=1 : 1).

(**7**). The 4-nitrobenzensulfonyl group of compound (**7**) was deprotected by treatment with PhSH and K_2CO_3 in DMF (*N*,*N*-dimethyformamide) to yield ZnAB, compound (**8**).

Fluorescence Properties of ZnAB with or without Zn^{2+} Under neutral conditions (pH 7.4), the final compound (**8**) (ZnAB) showed almost no fluorescence, and the fluorescence quantum yield was determined to be only 0.003. Upon addition of Zn^{2+}, the fluorescence intensity was increased by 30-fold (Fig. 1), and the fluorescence quantum yield was increased to 0.058. The wavelengths of the excitation and emission maxima were almost unchanged by Zn^{2+}: excitation at 499 nm and emission at 509 nm (Fig. 1).

Metal Ion Selectivity Metal ion selectivity was also examined. ZnAB was not influenced by other cations, such as Na^+, K^+, Ca^{2+}, and Mg^{2+}, which exist at high concentrations under physiological conditions, even at 2.5 mM, as shown in Fig. 2. These results are presumably due to the poor complexation of alkali metals or alkaline earth metals with the chelator of ZnAB. These cations also did not interfere with the Zn^{2+}-induced fluorescence enhancement. Among first-row transition metal cations, Mn^{2+}, Co^{2+}, Ni^{2+}, and Cu^{2+} induced a slight enhancement of the fluorescence intensity. Although ZnAB probably forms complexes with these metal cations, the fluorescence is weakened because of electron or energy transfer between the metal cations and the fluorophore, a known fluorescence quenching mechanism.[31,32]

Kinetic Analysis of the Complex Formation of Zn^{2+} Upon addition of various concentrations of Zn^{2+}, the fluores-

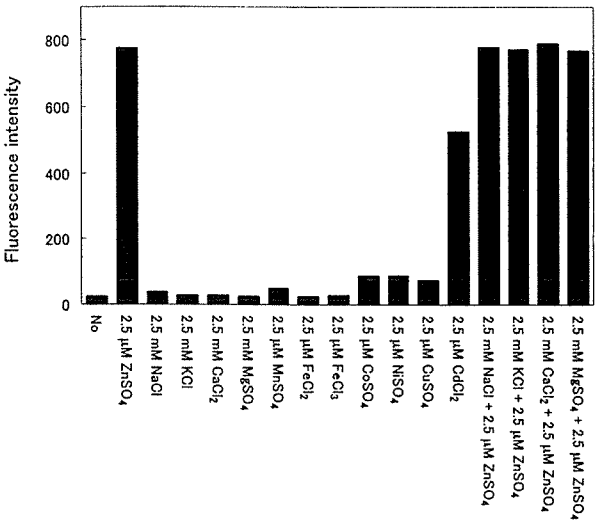

Fig. 2. The Relative Fluorescence Intensity of 2.5 μM ZnAB in the Presence of Various Cations

These data were measured at pH 7.4 (CH_3CN : 100 mM HEPES buffer (I= 0.1($NaNO_3$))=1 : 1).

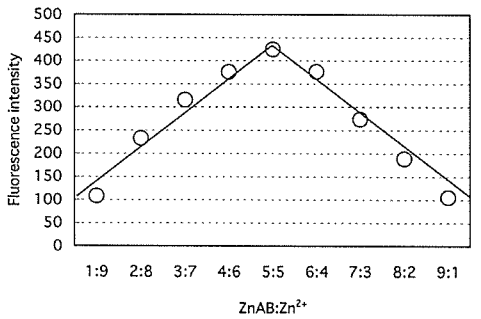

Fig. 3. Job's Plot for Zn^{2+} and ZnAB which Forms 1 : 1 Complex

The total $[Zn^{2+}]+[ZnAB]=5.0\ \mu M$.

cence intensity of ZnAB (2.5 μM) linearly increased up to a 1 : 1 [ZnAB]/[Zn^{2+}] ratio, and the fluorescence and absorption spectra did not change between 2.5 and 50 μM Zn^{2+} addition. Furthermore, a Job's plot analysis revealed maximum fluorescence obtained at a 1 : 1 ratio (Fig. 3). Next, we measured the association (k_{on}) rate constant of ZnAB at 25 °C, using a stopped-flow spectrofluorimeter. The k_{on} value of ZnAB was $2.43\times10^5\ M^{-1}\ s^{-1}$, implying that the complexation is sufficiently fast to detect an increase of Zn^{2+} concentration within a few hundred milliseconds.

The Effect of pH on the Fluorescence Intensity The fluorescence intensities (arbitrary unit) of the Zn^{2+} complex with ZnAB were 509.8, 490.6 and 468.1 at pH 5.48, 7.14 and 8.49, respectively. The fluorescence intensity of the Zn^{2+} complex with ZnAF-2, which is a fluorescein-based Zn^{2+} probe, extremely decreases below pH 7.0, whereas that of ZnAB hardly changed above pH 5.0. This insensitivity to pH of the fluorescence is useful for applications to living cells, where pH changes are caused by certain biological stimuli.

In conclusion, we have developed a new fluorescent Zn^{2+} sensor molecule, ZnAB, which possesses high selectivity under physiological-like conditions. In addition, ZnAB should be useful as a prototype of other BODIPY-based fluorescent probes for Zn^{2+}, whose absorption and emission maxima are shifted to longer wavelength by chemical modification.[33—36] Such derivatization would enable multicolor imaging, which can distinguish many compounds simultaneously owing to the differences of excitation or emission wavelength, and should be applicable to complex biological systems.

Experimental

All reagents and solvents were of the highest commercial quality and were used without further purification. Silica gel column chromatography was performed using Silica gel 60 (Merck). Aluminum oxide column chromatography was performed using Aluminum oxide 90 active neutral (Merck). Aluminum oxide TLC was performed using Aluminium oxide 60 F_{254} (Merck). ^{1}H-NMR spectra were recorded on a JEOL JNM-GX400 instrument at 400 MHz; δ values are given in ppm relative to tetramethylsilane. Mass spectra (MS) were measured with a JEOL MS700 mass spectrometer. Fluorescence spectroscopic studies were performed with a Shimadzu RF-5300. The slit width was 3.0 nm for both excitation and emission.

Synthesis of ZnAB (Chart 3). Preparation of Compound (2) To a solution of 4-acetamidebenzaldehyde (**1**) (10.0 g, 61.3 mmol) and 2,4-dimethylpyrrole (12.6 ml, 122.6 mmol) in 1000 ml of dichloromethane was added 100 μl of trifluoroacetic acid under an argon atmosphere, and the mixture was stirred for 4 h at room temperature. Then, a solution of DDQ (2,3-dichloro-5,6-dicyano-1,4-benzoquinone) (13.6 g, 61.3 mmol) in 25 ml of THF and 25 ml of dichloromethane was added dropwise to the mixture over 30 min. Stirring was continued at room temperature for 1 h, then the mixture was washed with water. The organic phase was dried over sodium sulfate and evaporated to dryness. The residue was chromatographed on aluminium oxide and eluted with acetone to afford compound (**2**) (4.54 g, 13.6 mmol). (yield 22%) ^{1}H-NMR (400 MHz, $CDCl_3$): δ 1.34 (6H, s), 2.21 (3H, s), 2.35 (6H, s), 5.89 (2H, s), 7.24 (2H, d, J=8.8 Hz), 7.61 (2H, d, J=8.8 Hz). MS (FAB$^+$ in m-nitrobenzyl alcohol as a matrix): m/z 334 ($(M+H)^+$).

Preparation of Compound (3) To a solution of compound (**2**) (3.77 g, 11.3 mmol) in 150 ml of methanol was added 150 ml of 1 N hydrochloric acid. The mixture was refluxed for 3 h, then cooled to room temperature, and extracted with dichloromethane. The organic phase was washed with water. The organic phase was dried over sodium sulfate and evaporated *in vacuo* to give compound (**3**) as a brown solid (3.30 g, 11.3 mmol). (yield 100%) ^{1}H-NMR (400 MHz, $CDCl_3$): δ 1.45 (6H, s), 2.36 (6H, s), 3.80 (2H, br), 5.91 (2H, s), 6.74 (2H, d, J=8.4 Hz), 7.05 (2H, d, J=8.4 Hz). MS (FAB$^+$ in m-nitrobenzyl alcohol as a matrix): m/z 292 ($(M+H)^+$).

Preparation of Compound (4) To a solution of compound (**3**) (3.27 g, 11.2 mmol) in 500 ml of dichloromethane was added diisopropylethylamine (26.5 ml, 152 mmol) under an argon atmosphere, and the mixture was stirred at room temperature for 15 min. Furthermore, BF_3–OEt_2 (28 ml, 211 mmol) was added, and the mixture was stirred for 40 min. The mixture was washed with water and 2 N NaOH aq., and the aqueous phase was extracted with dichloromethane. The organic phase was dried over sodium sulfate and evaporated to dryness. The residue was chromatographed on silica gel and eluted with dichloromethane to afford compound (**4**) (3.01 g, 8.87 mmol). (yield 79%) ^{1}H-NMR (400 MHz, $CDCl_3$): δ 1.49 (6H, s), 2.54 (6H, s), 3.94 (2H, br), 5.96 (2H. s), 6.79 (2H, dd, J=6.4, 1.6 Hz), 7.02 (2H, dd, J=6.4, 1.6 Hz). MS (FAB$^+$ in m-nitrobenzyl alcohol as a matrix): m/z 339 (M^+).

Preparation of Compound (5) To a solution of compound (**4**) (1.00 g, 2.95 mmol) and pyridine (0.48 ml, 5.90 mmol) in 20 ml of dichloromethane was added dropwise a solution of 4-nitrobenzenesulfonyl chloride (980.7 mg, 4.43 mmol) in 35 ml of dichloromethane over 10 min. The mixture was stirred overnight, then washed with water and brine, and dried over sodium sulfate. After evaporation of the dichloromethane, the residue was chromatographed on silica gel and eluted with dichloromethane to afford compound (**5**) (835 mg, 1.59 mmol). (yield 54%) ^{1}H-NMR (400 MHz, $CDCl_3$): δ 1.18 (6H, s), 2.42 (6H, s), 6.14 (2H, s), 7.25 (4H, m), 7.96 (2H, dd, J=8.8, 2.0 Hz), 8.34 (2H, dd, J=8.8, 2.0 Hz). MS (FAB$^+$ in m-nitrobenzyl alcohol as a matrix): m/z 524 (M^+).

Preparation of Compound (6) A mixture of compound (**5**) (604 mg, 1.15 mmol), cesium carbonate (450 mg, 1.38 mmol), 1,2-dibromoethane (1.00 ml, 11.5 mmol), and 20 ml of *N,N*-dimethylformamide was stirred at 80 °C for 2 h. After cooling to room temperature, the mixture was diluted with dichloromethane and washed with water and brine. The organic phase was dried over sodium sulfate and evaporated to dryness. The residue was

chromatographed on silica gel and eluted with dichloromethane to afford compound (**6**) (520 mg, 0.824 mmol). (yield 72%) ^{1}H-NMR (400 MHz, $CDCl_3$): δ 1.40 (6H, s) , 2.56 (6H, s), 3.45 (2H, t, J=6.8 Hz), 4.07 (2H, t, J=6.8 Hz), 6.02 (2H, s), 7.26 (2H, d, J=8.4 Hz), 7.33 (2H, d, J=8.4 Hz), 7.78 (2H, d, J=8.8 Hz), 8.30 (2H, d, J=8.8 Hz). MS (FAB$^+$ in *m*-nitrobenzyl alcohol as a matrix): *m/z* 630, 632 (M^+).

Preparation of Compound (7) A suspension of compound (**6**) (0.61 g, 0.966 mmol), 2,2′-dipicolylamine (0.52 ml, 2.90 mmol), potassium carbonate (0.33 g, 2.39 mmol), potassium iodide (0.41 g, 2.47 mmol) in 20 ml of acetonitrile was refluxed for 14 h. Acetonitrile was removed by evaporation, and the residue was diluted with 1 M potassium carbonate and extrated with dichloromethane. The organic phase was dried over sodium sulfate and evaporated to dryness. The crude product was chromatographed on silica gel (eluent: dichloromethane, dichloromethane–methanol 99.5 : 0.5 (v/v), 98 : 2 (v/v)) to afford compound (**7**) (0.19 g, 0.253 mmol). (yield 26%) ^{1}H-NMR (400 MHz, $CDCl_3$): δ 1.28 (6H, s), 2.55 (6H, s), 2.77 (2H, t, J=6.8 Hz), 3.88 (4H, s), 3.90 (2H, t, J=6.8 Hz), 5.99 (2H, s), 7.09 (2H, d, J=8.0 Hz), 7.18 (2H, d, J=8.0 Hz), 7.19 (2H, m), 7.54 (2H, d, J=8.0 Hz), 7.70 (2H, m), 7.71 (2H, d, J=8.8 Hz), 8.26 (2H, d, J=8.8 Hz), 8.52 (2H, d, J=4.8 Hz). MS (FAB$^+$ in *m*-nitrobenzyl alcohol as a matrix): *m/z* 750 ($(M+H)^+$)

Preparation of ZnAB, Compound (8). 8-[4-*N*-[*N*′,*N*′-Bis(2-pyridinylmethyl)-2-aminoethyl]aminophenyl]-1,3,5,7-tetramethyl-4,4-difluoro-4-bora-3a,4a-diaza-*s*-indacene To a suspension of compound (**7**) (66.6 mg, 0.0888 mmol) and potassium carbonate (61.4 mg, 0.444 mmol) in 5 ml of *N*,*N*-dimethylformamide was added thiophenol (30 μl, 0.293 mmol), and the mixture was stirred for 3 h at room temperature. *N*,*N*-Dimethylformamide was removed by evaporation, and the residue was diluted with dichloromethane, washed with water, and dried over sodium sulfate. The residue was purified by aluminum oxide TLC with dichloromethane to give a brown solid. The brown solid was dissolved in a small amount of diethyl ether and reprecipitated with hexane to afford ZnAB, compound (**8**) (13.5 mg, 0.0239 mmol) (yield 27%) ^{1}H-NMR (400 MHz, $CDCl_3$): δ 1.49 (6H, s), 2.54 (6H, s), 2.93 (2H, t, J=5.9 Hz), 3.17 (2H, t, J=5.9 Hz), 3.94 (4H, s), 5.96 (2H, s), 6.65 (2H, d, J=8.8 Hz), 6.97 (2H, d, J=8.8 Hz), 7.17 (2H, ddd, J=7.8, 4.9, 2.0 Hz), 7.44 (2H, d, J=7.3 Hz), 7.64 (2H, td, J=7.8, 7.3, 2.0 Hz), 8.58 (2H, m). MS (FAB$^+$ in *m*-nitrobenzyl alcohol as a matrix): *m/z* 565 ($(M+H)^+$).

Acknowledgments This study was supported in part by a grant for the Advanced and Innovational Research Program in Life Sciences from the Ministry of Education, Culture, Sports, Science and Technology the Japanese Government.

References

1) Vallee B. L., Falchuk K. H., *Physiol. Rev.*, **73**, 79—118 (1993).
2) Frederickson C. J., *Int. Rev. Neurobiol.*, **31**, 145—238 (1989).
3) Zalewski P. D., Millard S. H., Forbes I. J., Kapaniris O., Salvotinek A., Betts W. H., Ward A. D., Lincoln S. F., Mahadevan I., *J. Histochem. Cytochem.*, **42**, 877—884 (1994).
4) Zalewski P. D., Jian X., Soon L. L. L., Breed W. G., Seamark R. F., Lincoln S. F., Ward A. D., Sun F.-Z., *Reprod. Fertil. Dev.*, **8**, 1097—1105 (1996).
5) Qian W.-J., Aspinwall C. A., Battiste M. A., Kennedy R. T., *Anal. Chem.*, **72**, 711—717 (2000).
6) Matsushita K., Kitagawa K., Matsuyama T., Ohtsuki T., Taguchi A., Mandai K., Mabuchi T., Yagita Y., Yanagihara T., Matsumoto M., *Brain Res.*, **743**, 362—365 (1996).
7) Bush A. I., Pettingel W. H., Multhaup G., Paradis M. D., Vonsattel J.-P., Gusella J. F., Beyreuther K., Masters C. L., Tanzi R. E., *Science*, **265**, 1464—1467 (1994).
8) Frederickson C. J., Kasarskis E. J., Ringo D., Frederickson R. E., *J. Neurosci. Methods*, **20**, 91—103 (1987).
9) Savage D. D., Montano C. Y., Kasarskis E. J., *Brain Res.*, **496**, 257—267 (1989).
10) Zalewski P. D., Forbes I. J., Betts W. H., *Biochem. J.*, **296**, 403—408 (1993).
11) Zalewski P. D., Forbes I. J., Borlinghaus R., Betts W. H., Lincoln S. F., Ward A. D., *Chem. Biol.*, **1**, 153—161 (1994).
12) Budde T., Minta A., White J. A., Kay A. R., *Neuroscience*, **79**, 347—358 (1997).
13) Walkup G. K., Burdette S. C., Lippard S. J., Tsien R. Y., *J. Am. Chem. Soc.*, **122**, 5644—5645 (2000).
14) Hirano T., Kikuchi K., Urano Y., Higuchi T., Nagano T., *Angew. Chem. Int. Ed.*, **39**, 1052—1054 (2000).
15) Haugland R. P., "Handbook of Fluorescent Probes and Research Chemicals," 6th ed., Molecular Probes, Inc., Eugene, OR, 1996, pp. 531—540.
16) Woodroofe C. C., Lippard S. J., *J. Am. Chem. Soc.*, **125**, 11458—11459 (2003).
17) Hirano T., Kikuchi K., Urano Y., Higuchi T., Nagano T., *J. Am. Chem. Soc.* **122**, 12399—12400 (2000).
18) Hirano T., Kikuchi K., Urano Y., Nagano T., *J. Am. Chem. Soc.*, **124**, 6555—6562 (2002).
19) Maruyama S., Kikuchi K., Hirano T., Urano Y., Nagano T., *J. Am. Chem. Soc.*, **124**, 10650—10651 (2002).
20) Kojima H., Nakatsubo N., Kikuchi K., Kawahara S., Kirino Y., Nagoshi H., Hirata Y., Nagano T., *Anal. Chem.*, **70**, 2446—2453 (1998).
21) Kojima H., Urano Y., Kikuchi K., Higuchi T., Nagano T., *Angew. Chem. Int. Ed.*, **38**, 3209—3212 (1999).
22) Umezawa N., Tanaka K., Urano Y., Kikuchi K., Higuchi T., Nagano T., *Angew. Chem. Int. Ed.*, **38**, 2899—2901 (1999).
23) Tanaka K., Miura T., Umezawa N., Urano Y., Kikuchi K., Higuchi T., Nagano T., *J. Am. Chem. Soc.*, **123**, 2530—2536 (2001).
24) Rurack K., Kollmannsberger M., Daub J., *New J. Chem.*, **25**, 289—292 (2001).
25) Werner T., Huber C., Heinl S., Kollmannsberger M., Daub J., Wolfbeis O. S., *Fresenius J. Anal. Chem.*, **359**, 150—154 (1997).
26) Kollmannsberger M., Gareis T., Heinl S., Breu J., Daub J., *Angew. Chem. Int. Ed.*, **36**, 1333—1335 (1997).
27) Gee K. R., Rukavishnikov A., Rothe A., *Comb. Chem. High Throughput Screen.*, **6**, 363—366 (2003).
28) Rehm D., Weller A., *Isr. J. Chem.*, **8**, 259 (1970).
29) Miura T., Urano Y., Tanaka K., Nagano T., Ohkubo K., Fukuzumi S., *J. Am. Chem. Soc.*, **125**, 8666—8671 (2003).
30) Imahori H., Norieda H., Yamada H., Nishimura Y., Yamazaki I., Sakata Y., Fukuzumi S., *J. Am. Chem. Soc.*, **123**, 100—110 (2001).
31) Fabbrizzi L., Licchelli M., Pallavicini P., Sacchi D., Taglietti A., *Analyst* (London), **121**, 1763—1768 (1996).
32) de Silva A. P., Gunaratne H. Q. N., Gunnlaugsson T., Huxley A. J. M., McCoy C. P., Rademacher J. T., Rice T. E., *Chem. Rev.*, **97**, 1515—1566 (1997).
33) Burghart A., Kim H., Welch M. B., Thoresen L. H., Reibenspies J., Burgess K., Bergstroem F., Johansson L. S.-H., *J. Org. Chem.*, **64**, 7813—7819 (1999).
34) Chen J., Burghart A., Kovacs A. D., Burgess K., *J. Org. Chem.*, **65**, 2900—2906 (2000).
35) Rurack K., Kollmannsberger M., Daube J., *Angew. Chem. Int. Ed.*, **40**, 385—387 (2001).
36) Wada M., Ito S., Uno H., Murashima T., Ono N., Urano T., Urano Y., *Tetrahedron Lett.*, **42**, 6711—6713 (2001).

蛍光相関分光法(FCS)を用いた抗原抗体反応解析および検体検出

Antigen-Antibody-Reaction Analysis and Analyte Detection with Fluorescence Correlation Spectroscopy (FCS)

坂田啓司[*1]藤井文彦[*2]田村　守[*3]金城政孝[*4]

＊1 科学技術振興機構　研究成果活用プラザ北海道　生体ー分子計測研究室
＊2 科学技術振興機構　研究成果活用プラザ北海道　生体ー分子計測研究室
＊3 北海道大学　電子科学研究所　教授
＊4 北海道大学　電子科学研究所　助教授

シーエムシー出版刊『月刊バイオインダストリー2004年4月号』抜刷

蛍光相関分光法(FCS)を用いた抗原抗体反応解析および検体検出

特集 神経変性疾患研究の最前線

蛍光相関分光法（FCS）を用いた抗原抗体反応解析および検体検出

Antigen-Antibody-Reaction Analysis and Analyte Detection with Fluorescence Correlation Spectroscopy (FCS)

坂田啓司[*1] 藤井文彦[*2] 田村 守[*3] 金城政孝[*4]

1. はじめに

蛍光相関分光法（Fluorescence Correlation Spectroscopy，以下FCS）は，溶液中の蛍光分子のブラウン運動を利用し，分子の「大きさ」や「数」といった物理量を得る古くて新しい方法である[1~6]。

FCSの特徴は，溶液に含まれる蛍光分子の濃度や分子間相互作用を物理的な分離過程を経ずにほぼ実時間でモニタできることである。そのため，FCSを用いた検出系では，これまで主流となっていた生体分子検出系（例えばELISAなど）で必要であった煩雑なBound/Free分離過程を省くことができる。従って，短時間に多量のサンプルを高感度に，かつ自動的に測定することに向いている。

本稿では，特にFCSを用いた抗原抗体反応解析について報告する。

[*1]Hiroshi Sakata 科学技術振興機構 研究成果活用プラザ北海道 生体一分子計測研究室 研究員．筆者略歴：1999年大阪大学 工学部卒業，2001年同大学大学院 工学研究科修了．連絡先：〒060-0819 札幌市北区北19条西11丁目 Tel. 011-708-1614／Fax. 同左 (E-mail) hsakata@sapporo.jst-plaza.jp

[*2]Fumihiko Fujii 科学技術振興機構 研究成果活用プラザ北海道 生体一分子計測研究室．筆者略歴：1996年北海道大学 理学部卒業，1998年同大学大学院 理学研究科修了，2003年同 博士過程単位取得退学；連絡先：同上 (E-mail) ffujii@sapporo.jst-plaza.jp

[*3]Mamoru Tamura 北海道大学 電子科学研究所 教授．筆者略歴：1970年北海道大学大学院 理学研究科化学専攻 博士過程終了，1970~74年米国ペンシルバニア大学 医学部 博士研究員，1974年大阪大学 産業科学研究所 放射線高分子部門 助手，1978年北海道大学 応用電気研究所 生体物理部門 助教授，1988年同 教授，1992年同大学 電子科学研究所 超分子分光分野 教授．連絡先：〒060-0812 札幌市北区北12条西6丁目 Tel. 011-706-2410／Fax. 011-706-4964 (E-mail) mtamura@imd.es.hokudai.ac.jp

[*4]Masataka Kinjo 北海道大学 電子科学研究所 助教授．筆者略歴：1981年宇都宮大学 修士，1985年自治医科大学大学院修了，1985年北海道大学 応用電気研究所 助手，1997年同大学 電子科学研究所 助教授．連絡先：同上 Tel. 011-706-2890 (E-mail) kinjo@imd.es.hokudai.ac.jp

2. FCS 測定の原理

2.1 装　置

FCS 測定では，共焦点光学系を用いることにより，試料溶液の極微小領域（直径約 400nm，軸長約 2μm，体積～10^{-16}L）からの蛍光を検出している（図 1）。本稿では，FCS 測定に Carl Zeiss 社製の ConfoCor2 とオリンパス社製の MF 20 を用いた。測定は，波長 488nm で 30 秒間の測定を 3 回行った。後述する蛍光相互相関分光法による測定には MF20 を用いた。測定は，波長 488nm と 633nm で 120 秒間の測定を 3 回行った。

2.2 観測される蛍光強度の揺らぎ

観測領域は開放系であるため，蛍光分子はブラウン運動にしたがい領域内を出入りする。すると，観測領域中の分子の数はある値を中心に変動し，数の揺らぎが生じる。そして，この数の揺らぎに起因した蛍光強度の揺らぎが観測される[6]。

2.3 揺らぎの解析

揺らぎの信号から情報を引き出すために自己相関関数を用いる。FCS で用いる自己相関関数は式(1)で示される。

$$C(\tau)=1+\frac{1}{N}\left[\frac{1}{1+\tau/\tau_D}\right]\left[\frac{1}{1+(1/s)^2(\tau/\tau_D)}\right]^{1/2} \quad (1)$$

ここで，s は $s=z/\omega$ であり，観測領域の半径

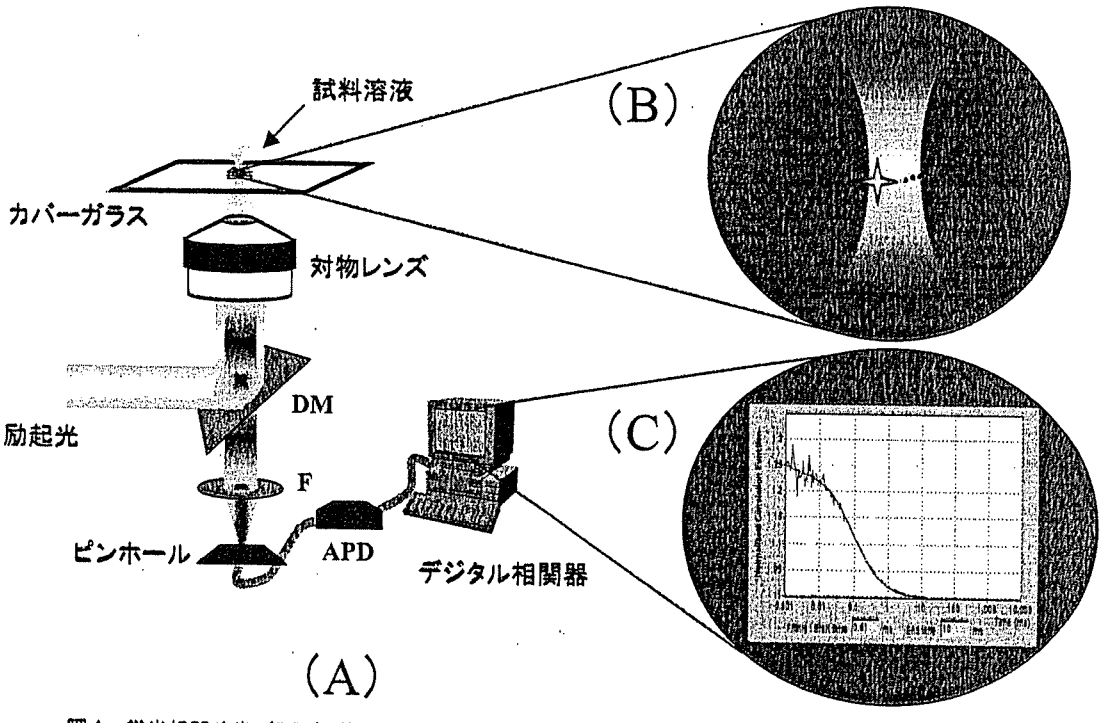

図 1　蛍光相関分光（FCS）装置(A)と観測領域の拡大(B)の模式図および蛍光相関解析後の相関曲線(C)

(A)レーザーからの励起光はダイクロイックミラー（DM）と対物レンズを経由してカバーガラス上の試料溶液に導かれる。蛍光発光はロングパスフィルター（F）を通り，共焦点上のピンホールで共焦点面以外のバックグラウンド光を取り除き，アバランシェフォトダイオード検出器（APD）へと導かれ，その信号はさらにデジタル相関器で解析される。

(B)対物レンズによって極限まで絞られた共焦点領域を，ブラウン運動している蛍光分子が通過する様子を示す。

(C)観測される蛍光強度の揺らぎを式(1)および(4)を用いて解析することで，分子の「数」や「大きさ」といった物理量が得られる。